INTERNATIONAL ATOMIC ENERGY AGENCY
UNITED NATIONS EDUCATIONAL, SCIENTIFIC AND CULTURAL ORGANIZATION

INTERNATIONAL CENTRE FOR THEORETICAL PHYSICS
34100 TRIESTE (ITALY) - P.O.B. 586 - MIRAMARE - STRADA COSTIERA 11 - TELEPHONE: 2240-1
CABLE: CENTRATOM - TELEX 460392-I

SMR/169 - 4

WORKSHOP ON OPTICAL FIBER COMMUNICATION
(24 February - 21 March 1986)

OPTICAL FIBER STRUCTURE AND FABRICATION

J.M. LEAL COSTA
Director of Technology
ABC-XTAL
Company of the ABC Group
Campinas, S.P.
Brazil

OPTICAL FIBER STRUCTURE AND FABRICATION

Lecture presented at the "Workshop on Optical Fiber Communication", 24/Feb-21/Mar/86, International Centre for Theoretical Physics, Trieste, Italy.

Author: Dr. José Muro Leal Costa
Director of Technology
ABC-XTAL
Company of the ABC Group
Campinas, S.P., Brazil

I - BASIC STRUCTURE

The optical fiber as a component in an optical communication system has the basic function of propagating light signals from the transmitting to the receiving end of the system. It is, therefore a waveguide for optical frequancy radiation.

Considering a simplified diagram of an optical communication system, as shown on Fig. 1, the basic requirements on the performance of an optical fiber can be determined.

TRANSPARENCY

The distances involved in telecommunication links are of the order of kilometers. Therefore the choice of proper materials for the fabrication of the fiber becomes critical from the point of view of transparency.

When this field of technology was started in the late 60's, the choice was made for silicate glasses since these materials were known for their high transparency at the visible and near infrared portions of the radiation spectrum.

The wavelengths for transmission in optical communications are governed partly by the feasibility of materials such as silicate glasses showing low attenuation at these wavelengths and, at the same time, by the availability of light sources emitting at these same wavelengths.

Today, after a considerable amount of work of R & D, semiconductor lasers based on GaAs substrates are available with lifetimes higher than 100 000 hours and allowing modulation frequencies of the order of GHz. These lasers emitt radiation on the range from 0.8 μm to 1.6 μm, with constitutes essentially the working portion of the radiation spectrum for optical communications presently.

Silicate glasses, that is, glasses which have silica (SiO_2) as a matrix, are known in the common day experience as transparent materials. Windows, bottles, television screens, light bulbs, etc., are a few of the large variety of applications of silicate glasses which use this advantage of light transparenry. But the degree of transparency necessary in an optical fiber for optical communication is extremely much higher than on these common applications. The windshield of an automobile, for example, which seems reasonably transparent, has an attenuation corresponding to about 100 000 dB/km. If the same glass was used to manufacture an optical fiber, the communication link couldn't be longer than 0.5 meter.

The level of attenuation necessary for making an optical communication link viable from the technical and economical aspects is of the order of a few dB/km.

Driven by a strong commercial interest of companies throughout the world, in less than two decades materials scientists have brought down the attenuation levels of feasible glasses by orders of magnitude.

The only medium which shows null attenuation to light is vacuum. The simple existence of matter causes attenuation of one sort or another. Pure silica glass is an amorphous oxide constituted of structural units of silicon (Si) atoms tetrahedrally surrounded by 4 oxygen (O) atoms. These units repeat themselves in an assymetrical and non periodic fashion , by sharing oxygens at the vertices of the tetrahedrals, as illustrated on figure 2. Even if it were possible to manufacture a 100% pure silica glass, this material would cause absorption of radiation due to the coupling of light energy to the oscillations of the Si-O atomic bonds about their equilibrium positions, and to electronic transitions within the atoms. These two mechanisms of absorption in silicate glasses occur in the far infrared and ultraviolet regions of the spectrum, respectively. Between these extremes, there is left a usable transmission "window" in the visible and near infrared region.

Another mechanism which contributes to the attenuation is due to light scattering whithin the material.The most significant form of scattering is due to compositional and density fluctuations which are frozen into the glass structure during cooling from the liquid state. This type of radiative attenuation, called Rayleigh scattering, is propotional to the inverse fourth power of the wavelength. Therefore, whithin the "window" previously determined by the high absorption regions, it becomes interesting to work at the highest possible values of wavelengths. These intrinsic loss mechanisms have been evaluted for glasses being commonly used today in the manufacturing of optical fibers, as shown in figure 3.

The manufacturing process, even by the sofisticated methods developed for the fabrication of optical fibers, necessarily cause the addition of impurities in the pure structure of the glass, which contribute with additional absorption effects. Considering the working region of the spectrum previously defined by the intrinsic absorption mechanisms, from 0.8 μm to 1.6 μm, the impurities relevant due to their contribution in absorption are the transition metal ions (Fe, Cu, Ni, Cr, V, Co, Mn) and hydroxyl groups (OH).

Although the contribution to absorption due to electronic transitions of metal ions are present across the whole working region of the spectrum, the techniques for manufacturing optical fibers presently have been able to bring the concentration of those ions down to very low acceptable levels. As shown on figure , these levels must be kept on the ppb (parts per billion) range!

The hydroxyl groups, which are formed and bonded to the structure by the presence of hydrogen in the glass, have fundamental stretching vibrations occurring between 2.7 μm and 4.2 μm, which is outside of the working region of the spectrum. But the harmonics of these vibrations fall whithin the range of interest, showing absorption peaks at 1.4 μm and 0.95 μm. As shown on figure 4, it is necessary to keep the OH concentration below 1 ppm in order to attain the 0.5 to 1 dB/km attenuation value at the higher wavelengths of the working spectrum.

WAVEGUIDE

The transmission medium of a optical telecommunication link must be able to guide the narrowly oriented beam of light generated by a semiconductor laser or light emitting diode. Although the air conducts light radiation reasonably well, aside from the common atmospheric perturbations such as rain and dust, the trajectory followed by a telecommunications link in a city or for long distances is never a perfect straight line.

Before the fabrication of the first optical fibers, some attempts were made for constructing light pipes. These pipes could guide light by means of a series of collimating lenses displaced at precise distances one from another, or by flowing gases through these pipes to have the same effect of lenses due to radial pressure differences, as illustrated on figure 5. It is not difficult to realize that the construction of the pipes was not feasible both from the technical and economical aspects.

Whatever method is used to guide a light wave, it must be based practically on the reflection or refraction of this wave. One of the well known mechanisms of light reflection is called "total internal reflection". This is the basic physical principle upon which is based the fabrication of optical fibers.

For a better understanding of this principle it is important to first analyse the phenomenon of light refraction. As shown on figure 6, as a light ray reaches the interface of two materials of different optical densities (represented by different indexes of refraction) it emerges from the denser into the less dense medium by changing its direction of propagation in such a way as to reach a critical situation, illustrated as the angle θc in the figure, where the refracted ray will be tangent to the interface. For angles of incidence higher than θc, there will be no refracted ray, occuring then a total internal reflection.

The physical law which governs this phenomenon of refraction, called Snell's law, states that

$$n_1 \sin \theta_1 = n_2 \sin \theta_2$$

where the angles θ_1 and θ_2 are shown on the figure.

To obtain the critical angle θc, θ_1 is let to be 90^o, giving,

$$\theta_c = \arcsin \frac{n_1}{n_2}$$

The optical fiber is then constructed as a cylindrical rod surrounded by an envelope of lower index of refraction. As illustrated on figure 7 this construction allows, by the same principle explained above, the guiding of light by a series of reflections at the interface of the two materials constituting the core and cladding of the optical fiber.

II - PHYSICAL PROPERTIES

MATERIAL PROPERTIES

The choice of silicate glasses to constitute the material used for fabrication of optical fibers is based not only on their transparency. At the time when this technology was started, there was already a considerable amount of literature about these glasses which allowed a certain degree of confidence that the proper behaviour could be obtained if these materials were made into hair thin fibers, later on cabled, launched into ducts below the earth or hung in the air, and kept on transmitting light pulses with very low attenuation for 20 years or more. Actually today no other economically feasible material is known by Science that is capable of having such a performance.

Glasses are materials which can neither be classified physically as solids nor liquids. At room temperature, their hardness or viscosity is certainly not liquid-like, but at the same time, the atomic structure is not periodic and symetrical like a solid should be. There is no universally accepted definition of glass. Commonly it is defined as a super-cooled liquid.

The amorphous atomic structure allows the property of isotropy, that is, indifferent behaviour regarding the relative direction by which its physical properties are analyzed. Therefore, its optical transmission, thermomechanical behaviour, stress relaxation, etc, are independent relatively to the orientation on its structure. The absence of these properties could be disastrous in a material from which an optical fiber were made.

Models such as the one illustrated on figure 8 have been proposed for the atomic structure of oxide glasses. It is easy to observe from the figure that the isotropic characteristic is derived from the chaotic arrangement of atoms in the structure.

The liquid like atomic arrangement found in oxide glasses is attained when it is cooled from the liquid state, as illustrated on figure 9. At the glass transition, analogous to a process of solidification, the structure is "frozen" due to very long relaxation times. Glasses, therefore, are not in a state of complete thermodynamic equilibrium. This does not constitute a practical problem because the relaxation times at room temperature are such that no observable structural differences tending towards crystalization may occur in thousands of years.

Aside from the isotropic characteristic of glasses, these materials allow compositions which are not stoichiometric in nature, that is, they can be prepared as solutions with a large degree of freedom in choosing glass compositions with silica as a matrix and a variety of other oxides as dopants. This property is essential for optical fiber manufacturing, since there is a necessity of changing the index of refraction of the glasses in the making of the core and cladding of the fiber, as already mentioned before.

As illustrated in figure 10, there is a large range of dopant concentrations, which can either increase or decrease the index of refraction of pure silica, still maintaining its glassy structure.

Another important physical characteristic of silicate glasses is its mechanical strength. Glasses are certainly not known by common day experience as strong materials. Actually, the opposite is what every one has in mind when thinking about glass, as evidenced by the glass champagne signs stamped on carton boxes used for shipping fragile goods.

The mechanical strength of any material is a function primarily of its interatomic binding forces. Due to the structure of silica, these forces are reasonably high as compared to other materials. But silicate glasses have the disadvantage of being brittle. Other materials, as illustrated on figure 11, when subjected to stress release their tension by deforming plastically. Glasses have no plastic behaviour, being forced therefore to act mechanically only on an elastic regime.

Since plastic deformation is forbiden, when a mechanical shock is applied to a glassy material, the tension therefore created cannot be absorbed as it happens with a metallic material which deforms plastically releasing consequently the energy contained in that shock. The end result is an enormous concentration of stresses on any defect existing on the glass. On optical fibers these defects are usually on the surface.

Models as illustrated on figure 12 have been created for the mechanical failure of glasses in general. A surface crack theoretically in the shape of an elipse, has the net effect of greatly amplifying the stresses at the tip of the crack, reaching values which are then higher than the intrinsic strength of the glass, finally causing failure.

A theorical model for this amplification effect can be expressed as

$$\sigma_{effective} = 2\,\sigma \left[\frac{a}{\rho}\right]^{1/2}$$

where, as illustrated on figure 12, $\sigma_{effective}$ is the stress at the tip of the crack, σ is the applied stress, a is the semi-major axis of the elipse and ρ is the radius of curvature at the tip.

Optical fibers are coated with adequate polymers during the process of manufacturing with the objective of preserving the mechanical strength of the glass. The coating protects the surface of the fiber, preventing the mechanical or chemical attack from external agents.

DIMENSIONS

The geometrical parameters of optical fibers have been determined from a combination of technical and practical conveniences. Due to the specific and very convenient rheological behaviour of silicate glasses at high temperatures, allowed by surface tension and viscosity characteristics, a glass fiber can be fabricated with a large range of diameters, as illustrated on fig. 13. A higher limit for the diameter of the fiber is determined essentially from the necessity of flexibility for further processing and handling of the fibers in general. As illustrated an figure 14, when the fiber is bent on a circle of radius of curvature R, the inner half of the cross-section of the fiber is subjected to compression and the outer half to tension.

The highest value of tension at the outer surface of the fiber can be calculated as

$$\sigma = E\left[\frac{1}{2\left[\frac{R}{\phi}\right]+1}\right]$$

where E is the modulus of elasticity and ϕ the diameter of the fiber. Assuming a value for the tension of rupture as approximately 400 kgf/mm^2 and E = 7 x 10^3 kgf/mm^2, we can find practical values for the radius of curvature R_R as a function of diameters of the fiber, as illustrated on figure 14. With a diameter of around 400 µm, the fiber is already getting too stiff to handle.

The lower limit for the diameter of the core, or the nucleus of the fiber, which is the optically "active" region of the fiber, is determined by the efficient coupling of light from the radiation source into the fiber. As illustrated on figure 15, semiconductor lasers emitt radiation on a solid angle pattern with origin on the active region of the laser, which has a dimension of about 10 µm. Therefore this defines the lower limit for the diameter of the nucleus.

With these considerations, and also fabrication characteristics, the outside diameter of optical fibers for telecommunications has been standardized as 125 ± 3 µm. In the specific case of "graded index" fibers, the diameter of the nucleus has been also standardized as 50 ± 3 µm. "Monomode fibers" have nuclei with diameters in the range of 10 µm.

Other geometrical parameters, such as non-concentricity of nucleus and cladding, and non-circularity of nucleus, have been standardized as illustrated on figure 16. These parameters are fundamental for controlling optical losses on splicing operations and connector application.

NUMERICAL APERTURE

The principle of total internal reflection upon which the operation of an optical fiber is based, as illustrated before, defines a critical angle for the reflections occuring at the interface of nucleus and cladding of the fiber. From the point of view of an efficient coupling of light with the fiber, it is interesting to have a critical angle as large as possible. Similarly to lenses, a parameter is needed to characterize this coupling capacity from an outside source.

As illustrated on figure 17, when a light ray coming from an outside source is launched into the fiber making an angle θ with the axis it is refracted into the fiber with an angle θ_1, given by Snell's law as

$$n' \sin\theta = n_1 \sin\theta_1,$$

where n' and n_1 are, respectively the indexes of refraction of the fluid outside the fiber (usually air) and of the nucleus.

After propagation in the nucleus, the ray reaches the interface with the cladding and, considering the critical situation of reflection, makes an angle

$$\theta_C = \arcsin\left[\frac{n_2}{n_1}\right]$$

with the interface, as illustrated on figure 17, and previously demonstrated from the principle of total internal reflection in the optical fiber. In this case, the angle θ is the maximum possible angle for launching light into the fiber avoiding refraction from the nucleus out to the cladding.

The parameter called numerical aperture, defined as the sin θ, represents the capacity of an optical fiber to couple light into its nucleus. It is easily shown from the angular relations in the figure that

$$N.A. = [n_1^2 - n_2^2]^{1/2},$$

where n' (air) has been set equal to unity.

It can be shown that the coupled power is directly proportional to the square of the numerical aperture. Graded index fibers used today in telecommunications have numerical apertures around 0.21, which corresponds to an acceptance angle θ of approximately 12°.

TENSILE STRENGTH

The mechanical strength of an optical fiber is an important parameter on the life-time of optical systems, and in some cases as submarine systems for example, a critical one.

Rupture on fibers can occur in two ways. On a short time basis, the existence of cracks on the surface as already described, can propagate radially throught the fiber and cause breakage. This could occur during cabling or installation in the field, where the cable may have to be pulled throught ducts by considerable pulling forces. On a long time basis, a mechanism of failure called static fatigue can also take place, due to stress-induced growth of surface flaws in the presence of moisture. As illustrated on figure 18, both mechanisms are due to the propagation of cracks from the fiber surface.

The mechanism of failure on a short time basis is statistical in nature. It is based theoretically on a "weakest link" model, where the failure occurs at the weakest link of a long chain. A probabilistic Weibull distribution expressed as

$$f = 1 - \exp -\left[\frac{L}{L_0}\left[\frac{\sigma_f}{\sigma_c}\right]^m\right],$$

can be used to explain the data obtained when small samples of the optical fiber are taken to rupture on a short time.

In the expression above, f stands for the cumulative probability of failure, L is the length of the fiber, σ_f is the stress at failure and σ_c, L_0 and m are constants.

The direct dependence of f with the length L of the fiber comes from the fact that the longer the fiber, the higher the surface area and therefore the larger the probability of existing cracks at the surface. A typical Weibull plot is shown in figure 18, expressing the cumulative probability of failure at or above the tension of rupture of a 125 μm diameter fiber coated with silicone.

The theoretical models proposed for explaining the mechanism of failure by static fatigue rely on studies of crack propagation as a function of time. The data obtained from those studies apparently seem to fit the expression

$$\log t = K_1\sigma + K_2,$$

where t is the time to failure, σ is the applied stress and K_1 and K_2 are constants. A typical result is shown on figure 18 for a 125 μm diameter fiber coated with silicone and nylon. Extrapolation from these data to times of the order of 20 years or more can only tell us that the cabled fiber after installation has to be stressed at a level well below 10 K.

ATTENUATION

With the technologies commercially available today for the fabrication of transmitters and receivers, a typical optical communication system allows a total loss of about 40 dB from the semiconductor laser to the fotodetector.

Splicing techniques have been developed allowing losses of the order of 0.2 dB and connectors are also available with losses smaller than 1 dB.

Considering a typical intra-city telecommunications link of about 10 km, as illustrated on figure 19, after a 2 dB loss due to connectors and another 2 dB due to splicing (these values vary of course depending on the specific conditions of the system), we are left with 36 dB allowed for the attenuation of the optical fiber link. Usually around 6 dB are conservatively left for aging of the whole system. Therefore the optical fiber itself should show attenuation less than around 3 dB/km.

The attenuation in an optical fiber has a spectral distribuition as already mentioned before. As illustrated on figure 20, the various effects of absorption and scattering losses result in a transmission "window" in the near infrared, where semiconductor lasers based on gallium arsenide (GaAs) have their transmission wavelengths.

Combining a number of factors involving the availability of lasers, low fiber transmission attenuation and other effects related to the transmission bandwidth, there are today three main working wavelengths; 0.85 μm, 1.3μm and 1.55μm.

The attenuation at 1.3 μm and 1.55 μm has in the past years decreased considerably to practically intrinsic values of about 0.4 dB/km and 0.25 dB/km, respectively. This has been possible by fabrication techniques that control the concentration of OH^- radicals to below ppm levels.

DISPERSION

Ideally, the optical fiber as the transmission medium of a communication system should reconstruct optical signals at the output end with exactly the same form as at the input.

As we have already analyzed, the intensity of the signal is decreased due to intrinsic loss mechanisms. But aside from the attenuation factor, an optical signal is distorted in the fiber due to dispersion effects. Light propagates in the fiber as guided electromagnetic waves with different modes of propagation. Each mode can be approximately analyzed as a plane transverse wave propagating in a specific direction in relation to the axis of the fiber. In a simplified view each mode can be associated to a light ray propagating at a specific angle to the fiber axis,as illustrated on figure 21.

If the material composing the nucleus of the fiber is homogeneous, the index of refration has the same value at all points in the nucleus and, consequently, all rays propagate with the same velocity. Since their paths are different, there is a time delay between the individual rays (modes) and when they reconstruct the input signal at the exit of the fiber, there will necessarily be a time enlargement of the signal.

This mechanism of time distortion is called modal dispersion and, basically because of it, optical fibers are classified into two main types: multimode and monomode. As the names indicate, the classification implies the transmission by means of various modes or a single one.

Multimode fibers are further classified in two types: step index and graded index. As illustrated on figure 22, this nomenclature is based on the profile of the index of refraction through a diameter of the cross-section of the fiber. The profile on step-index fibers resemble a step, and graded index fibers have a gradually variable index from the axis out to the interface with the cladding in an approximately parabolic shape.

Modal dispersion in multimode step index fibers is of the order of 50 ns/km, that is, after propagating for a kilometer in the fiber, a light pulse is spread in time by 50 ns at its half intensity, where it is conventionally measured.This is too high for telecommunication purposes, which involves transmission rates of hundreds of million of pulses per second, as in a pulse code modulation (PCM) system. As illustrated on figure 23, the time spread due to modal dispersion causes an overlap of the outcoming pulses making it impossible to identify these pulses with a reasonable degree of confidence.

To overcome this problem, modal dispersion has to be diminished to minimum possible values. This is done on a multimode fiber, by varying the index of refraction in such a way as to compensate with a higher velocity, larger distances of propagation. Graded index fibers are therefore fabricated with this main objective. Theoretically, modal dispersion would be very close to zero, meaning almost infinite bandwidth for transmission. In practice though, it is very difficult, if not impossible, to obtain a perfectly graded fiber. But the

modal dispersion is reduced to values around 0.5 ns/km, making it feasable for transmission rates of 45 Mbit/sec (480 telephone channels) over distances of the order of 15 kilometers.

An alternative solution to modal dispersion in optical fibers is to eliminate it completely, by allowing a single ray (mode) to propagate in the fiber. This type of fiber, called monomode, is constructed by a combined small diameter nucleus and small index difference between nucleus and cladding. In this type of fiber, as illustrated on figure 24, there is the necessity of an intermediate "optical cladding" of very low attenuation, due to the propagation of ligth outside of the nucleus of the fiber. The concept of rays from Geometrical Optics is unsufficient to explain propagation in monomode fibers, because the field of the fundamental mode extends out of the nucleus well into the optical cladding. But the ray analysis allows the interpretation of zero modal dispersion due to the absence of all other rays but the one propagating along the axis of the fiber.

Aside from modal dispersion there are other mechanisms of time distortion which are smaller in magnitude but become relevant when the modal dispersion is null, as in the case of monomode fibers. These mechanisms can be considered as intramodal and depend not only on the fiber itself but also on the spectral width of emission of the source.

No source is perfectly monochromatic, that is, the emitted radiation will allways have more than one wavelength component. Semiconductor laser based on GaAs, for example, have spectral widths of the order of a few nm's, which is very small but sufficient to cause what is called material and waveguide dispersion.

The time delay τ of a light pulse propagating in a monomode fiber, therefore with nonexistent modal dispersion, can be shown to be expressed by

$$\tau = -L \frac{\lambda^2}{2\pi c} \frac{d\beta}{d\lambda},$$

where L is the length of fiber, c the speed of light and β the propagation constant.

Material dispersion effects are calculated assuming only a dependence of β on the index of refraction n which changes as a function of wavelength λ, as illustred on figure 25. The specific material used for fabricating the fiber will of course determine the exact variation of n with λ. For a silica glass the n versus λ curve shows an inflection point at approximately 1.3 μm. The variation of the time delay of a pulse with the wavelength for distance L travelled in the fiber, assuming only a n dependence of β, the material dispersion, is given by

$$\frac{1}{L} \frac{d\tau_m}{d\lambda} = \frac{-1}{c} \lambda \frac{d^2 n}{d\lambda^2}$$

where τ was assumed to be equal to $\frac{2\pi n}{\lambda}$. As illustrated on figure 25, it will be zero approximately at 1.3 μm.

Waveguide dispersion effects are calculated assuming the index of refraction n to be a constant. The function β can then be considered as a function of a waveguiding parameter, called the normalized frequency V, and expressed as

$$V = \frac{2\pi a}{\lambda} [2n\Delta n]^{\frac{1}{2}},$$

where a is the radius of the nucleus of the fiber.

The waveguide dispersion can then be expressed as

$$\frac{1}{L} \frac{d\tau_w}{d\lambda} = -\frac{V^2}{2\pi c} \frac{d^2\beta}{dV^2}$$

As illustrated on figure 26, the relative value of this effect is small when compared to material dispersion, except at the region when the latter nears zero.

The combined effects of material and waveguide dispersion, called chromatic dispersion, has been the subject of considerable work lately. As indicated on figure 26, the relative contributions of those effects can lead to minimum dispersion, allowing very large bandwidths.

III - FABRICATION TECHNIQUES

The fabrication of optical fibers constituted a major technological problem in the early 70's. The challenge was considerable mainly because the techniques available then for glass making could not allow the very low light attenuation levels necessary for optical communications.

Conventional fusing techniques had the intrinsic problem of adding light absorbing impurities to the glass melt aside from the ones already present in the solid raw materials.

An ideal optical fiber should transmit light pulses along its length reconstructing these pulses at the exit end in exactly the same form as at the input. To fabricate a fiber that approximates as close as possible to the disired theoretical structure a series of problems have to be overcome, as illustrated on figure 27.

Due to the wave nature of light propagation, a lossy cladding will affect the attenuation of the core-guided modes. The existence of bubbles in the cladding and irregularities at the core-cladding interface distort the propagation of modes in the core. Deviations in the index profile from the theoretically predicted shape causes excessive mode dispersion, thus decreasing the bandwidth. Variations in diameter and deviations from cylindrical symmetry cause excessive splicing losses.

Light attenuation is critically dependent on Rayleigh scattering from compo sition fluctuations and absorption from metalic impurities or OH^- radicals. Finally, the mechanical strength of the fiber is severely affected by the existence of cracks at the surface of the cladding.

To overcome all these problems the technique which has proven most successfull is generally called chemical vapour deposition (CVD). Other techniques, involving the conventional fusing of multicomponent silicate glasses have been used but are severely limited on the achievable purity of the glasses necessary for low attenuation fibers. There are many variations of the basic CVD technique, known in the literature as modified chemical vapour deposition (MCVD), outside vapour phase oxidation (OVPO), vapour phase axial deposition (VAD), etc.

All these techniques have in common the basic method of first obtaining small submicroscopical glass particles by the oxidation of chloride vapours at temperatures above 1000°C. As illustrated on figure 28, the particles are subsequently sintered forming a homogeneous glass layers. To control the index of refraction other chlorides are also oxidized by an adequate proportion and then incorporated into the basic silica glass matrix.

The fabrication technique of CVD and all its variations, involve for practical reasons a two stage process since a glass fiber cannot be directly obtained. Thus, on a first stage, a glass rod is fabricated with all the structural characteristics of the optical fiber into which it will be transformed by fusion and pulling on a second stage, as illustrated on figure 29. The fabri

cation of the preform is the more critical stage of the process from the technological point of view.

The variations of the CVD technique differ from each other on the method of obtaining the preforms. As illustrated on figure 30, vapours of the chlorides are obtained by bubbling oxygen in sealed containers where the chlorides are held on a liquid state. High precision flowmeters control the outcoming flux of the vapours on the range of ml/min and the mixture of adequate proportions is fed to the preform manufacturing set-up.

On the MCVD process, oxydation of the chlorides occurs inside a rotating silica glass tube with internal diameter around 18 mm and about 1 m in length. The tube is heated from the outside by means of a traversing O_2-H_2 torch which takes the temperature at the inside of the tube to about 1300°C. The soot formed by the glass particles originated from the oxydation reaction is deposited on the inner surface of the tube and subsequently sintered forming a thin glass layer of approximately 10 µm thickness. When the end of the tube is reached, the gas torch returns to the original position at a faster speed so that no deposition occurs during that step, due to unsufficient temperature for the oxydation reaction. A new layer is then deposited on top of the previous one, and this build up process repeats until a necessary quantity of glass is deposited to constitute the nucleus of the preform. This will depend on the geometry of the starting silica tube, since the relative nucleus to cladding diameter ratio has to be fixed for subsequent fiber pulling.

The deposition process is then interrupted, the temperature at the surface of the tube is raised to about 2000°C and, by surface tension effects, the composite tube collapses to a solid rod. By an adequate variation at each deposition step of the relative concentration of components such as GeO_2, which vary the index of refraction, an adequate radial index profile is build up in the preform, layer by layer, as indicated on figure 31. Preforms for graded index fibers are thus obtained by gradually increasing the dopant concentration on an approximately linear variation. After the geometric transformation occurring on the colapsing step it will result an index profile with a near parabolic shape. For monomode fibers, an optical cladding is first deposited with a fixed dopant concentration and the nucleus of the fiber results from the deposition of only a few number of layers with slightly higher index of refraction.

A slight variation of the MCVD process, called plasma induced modified chemical vapour deposition, utilizes a microwave generator in the form of a radio frequency coil through which a stationary silica tube is positioned. The pressure inside the tube is held at low values (1-100 mmHg) and the plasma created by the microwave radiation (~3 GHz) supplies the energy for the oxidation reaction. The microwave cavity is moved at fast speeds when compared to the MCVD process, allowing the deposition of a much larger number of deposited layers. The spatial resolution on the profile is therefore much higher, which is convenient specially for graded index fibers.

The OVPO process, as illustrated on figure 30, utilizes the same basic idea of building up the index profile, layer by layer but the deposition is made starting at the surface of a mandrel around which a porous glass preform is manufacttured. The variation of dopant concentration is made in the opposite way as to the MCVD process, that is, it is gradually decreased in the vapour flux fed to a gas burner. The glass soot generated by flame hydrolysis at the burner is directed towards the mandrel where it is collected. At the end of deposition the mandrel is removed and the porous preform is sintered in a furnace held at 1400°C-1700°C, through which the preform traverses at a slow speed similarly to a zone refining process. After being properly cladded by a silica tube, the preform is then ready for fiber pulling.

The basic difference of the VAD process as compared to others is the fact that the index profile of the preform is built up at a single deposition step. The glass particles blown out of the gas torch follow different paths according to their compositions before adhering to the bottom of the vertically held silica rod at the start of the process. The net result of the tranverse diffusion of the particles is a radial variation in composition, and thus in the index of refraction, which can be controlled to give a proper profile. The main advantage of this process is that it allows a continuous fabrication of the preforms, not limited in length as in the case of the other processes.

The transformation of the preforms in the final shape of the optical fiber is carried on a pulling structure, where the preform is heated at its bottom end, continously pulled into a fiber, and then rolled on a drum.

A series of processing parameters have to be carefully controlled to assure that the quality of the fiber is not deteriorated. As illustrated on figure 32, the final geometry of the optical fiber is determined at the heating zone, where the bottom of the preform and the fiber are in a liquid state at about 2000°C. This is a critical zone of the pulling process regarding the final outer diameter of the optical fiber. To assure the very small tolerances allowed on the fiber diameter (± 3 µm), the heating zone has to have very high thermal stability and cylindrical symmetry. Since the temperature involved in pulling high silica fibers are very high, conventional wire resistance furnaces cannot be used. The most commonly used furnaces have graphite resistance elements or zirconia magnetic induction elements.

As soon as the fiber leaves the heating zone it is cooled by convection with the air, goes through the glass transition temperature and solidifies into its final glassy structure. Its outer diameter is then controlled by a non-contact laser scanning micrometer which measures the shadow created by the fiber on a photodetector at the opposite side of the fiber. On this region the fiber is kept on a filtered laminar flow atmosphere to avoid contamination of its surface in order to preserve its mechanical strength.

The naked fiber is then coated by passing it through a crucible which is filled with a liquid polymer solution. The main function of this primary coating is to prevent any damage to the surface of the fiber due to handling

or its simple exposure to the ambient atmosphere. The polymers mostly used for primary coating today are silicone and acrylate resins. The first has the additional advantage of serving also as a mechanical buffer. But the curing of this resin is done by heat conduction, which limits the speed of pulling of the fiber. Acrylic resins have the advantage of allowing less variation on the mechanical strength of the fiber along its length and since this resin can be cured by ultraviolet radiation, the speed of pulling can be much higher as compared with silicone coating. The polymer is cured further down on the pulling structure by passing the fiber through a resistance wire furnace or an altraviolet radiation generator depending on the polymer used.

Before winding on the take-up drum, the tension of pulling is monitored by a transducer coupled to a system of pulleys. The speed of pulling, around 1 m/sec for silicone coating and 5 m/sec for acrylate coating, is varied on a feed back mechanism with the laser micrometer, to keep the fiber diameter within the required tolerances.

SUGGESTED READING

The publications listed below should serve as a small starting reading material for optical fiber properties and fabrication techniques.

- TECHNICAL DIGEST, EUROPEAN CONFERENCE ON OPTICAL COMMUNICATIONS, I (1975) TRHOUGH XI (1985), organized in cooperation with the Institute of Electrical Engineers of England, Prance, Germany, Italy, Holand, Switzerland.

- OPTICAL FIBRE COMMUNICATION, TECHNICAL STAFF OF CSELT, 1980, edited by CSELT, Via G. Reiss Romoli, 274, 10148, Torino, Italy.

- LIST OF TECHNICAL PAPERS ON OPTICAL FIBERS, 1980, IBARAKI ELECTRICAL COMMUNICATION LABORATORY, N.T.T., JAPAN.

- PROPERTIES AND APPLICATIONS OF GLASS, HAROLD RAWSON, 1980, ELSEVIER SCIENTIFIC PUBLISHING COMPANY, 335 JAN VAN GALENSTRAAT, P.O. BOX 211, 1000 AE, AMSTERDAM, THE NETHERLANDS.

- OPTICAL FIBRE COMMUNICATION SYSTEMS, C.P. SANDBANK, 1981, JOHN WYLEY AND SONS, LTD., NEW YORK.

- OPTICAL FIBRES FOR TRANSMISSION, JOHN E. MIDWINTER, 1979, JOHN WYLEY AND SONS, INC., NEW YORK.

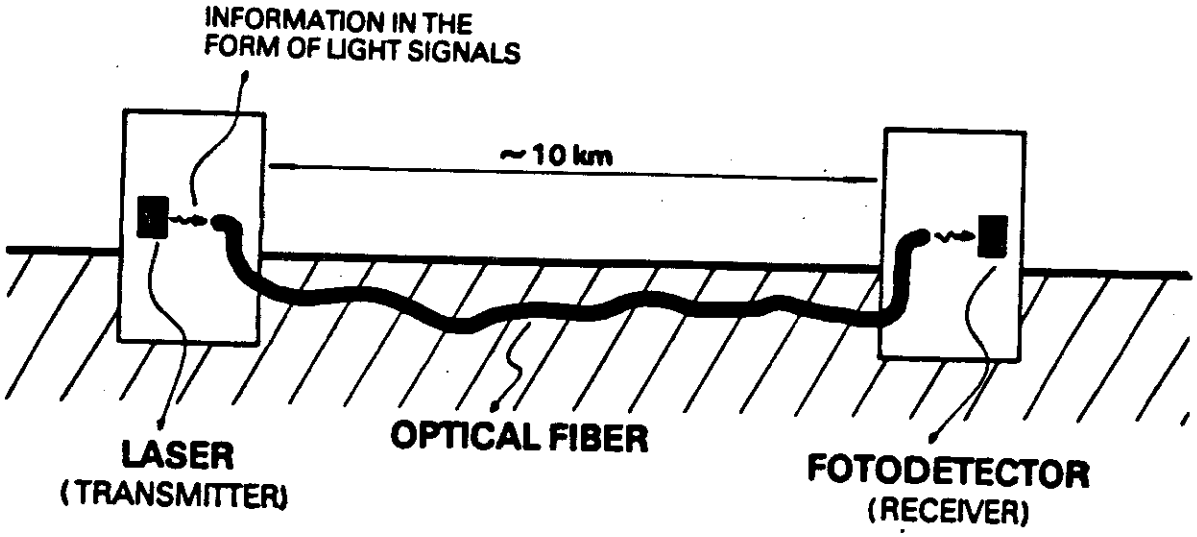

FIGURE 1

abc xtal

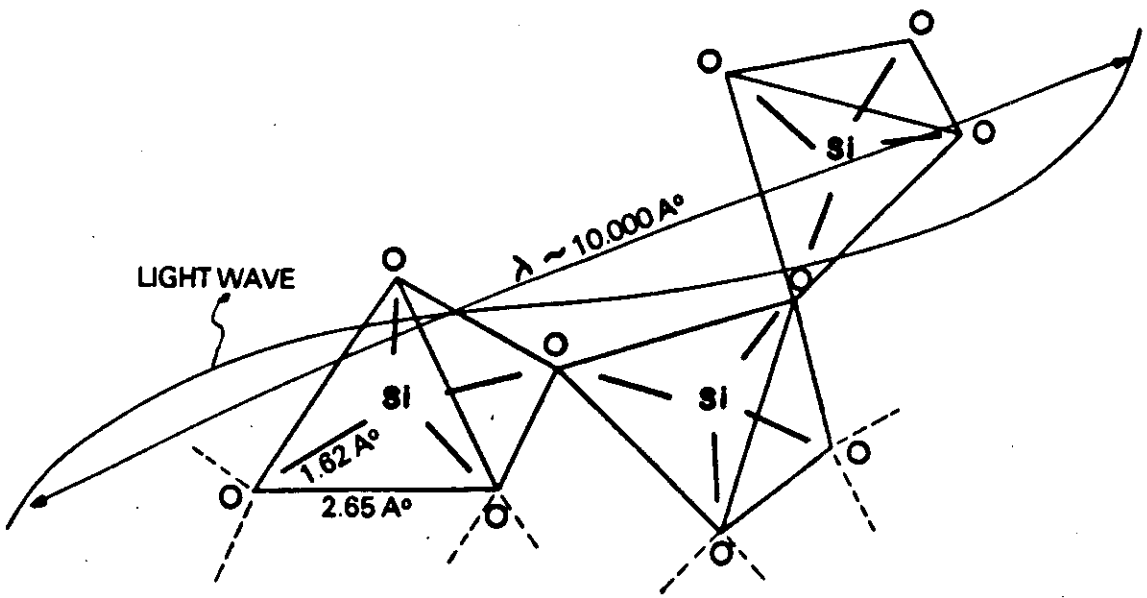

ABSORPTION LOSS
- Si-O
- ELECTRONIC TRANSITIONS

SCATTERING LOSS $\sim \frac{1}{\lambda^4}$

FIGURE 2

abc xtal

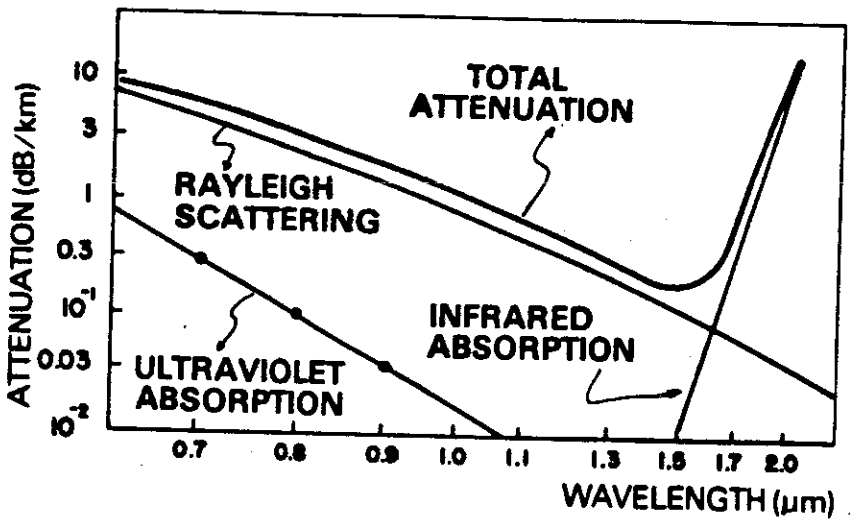

FIGURE 3

abc xtal

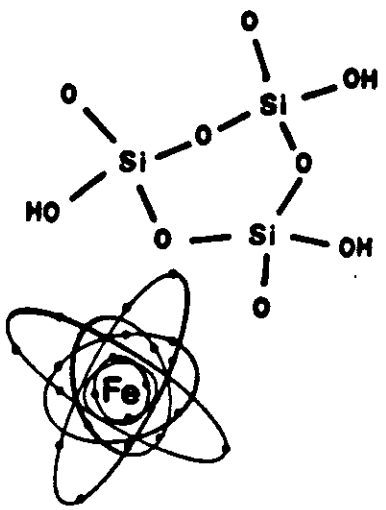

IMPURITY	ABSORPTION (dB/km/ppb)
OH	0.001 (at 0.95 μm) 0.04 (at 1.4 μm)
Fe	<0.2 (0.8 - 1.6 μm)
Cu	<0.2 (08 - 1.6 μm)
Cr	1.5 (at 0.8 μm) 0.8 (at 1.6 μm)
V	2.5 (at 0.8 μm) 0.2 (at 1.6 μm)

FIGURE 4

abc xtal

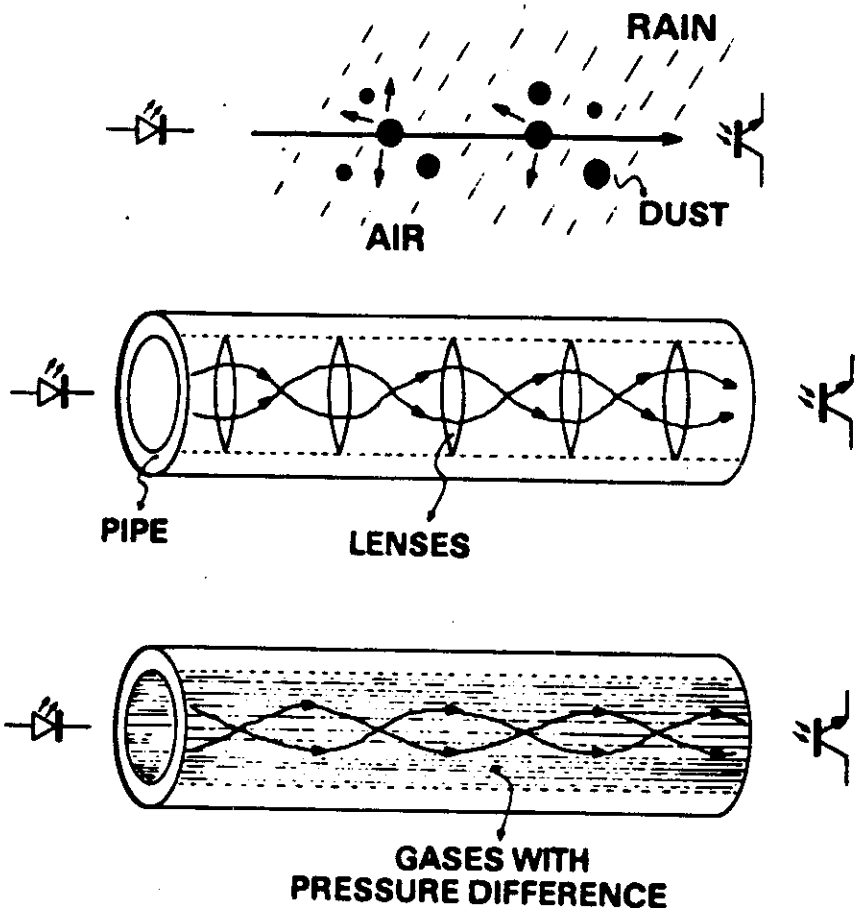

FIGURE 5

abc xtal

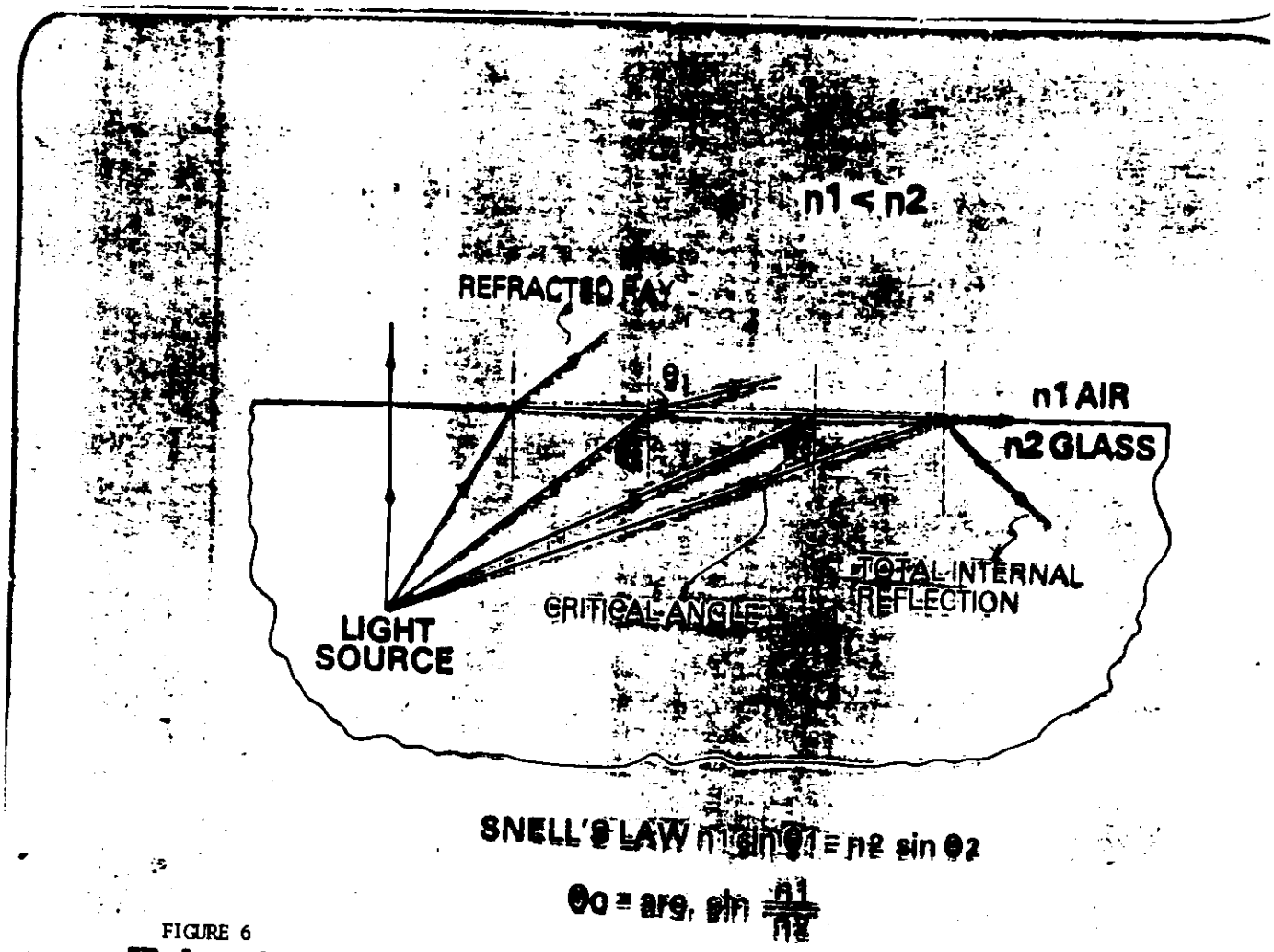

FIGURE 6

abc xtal

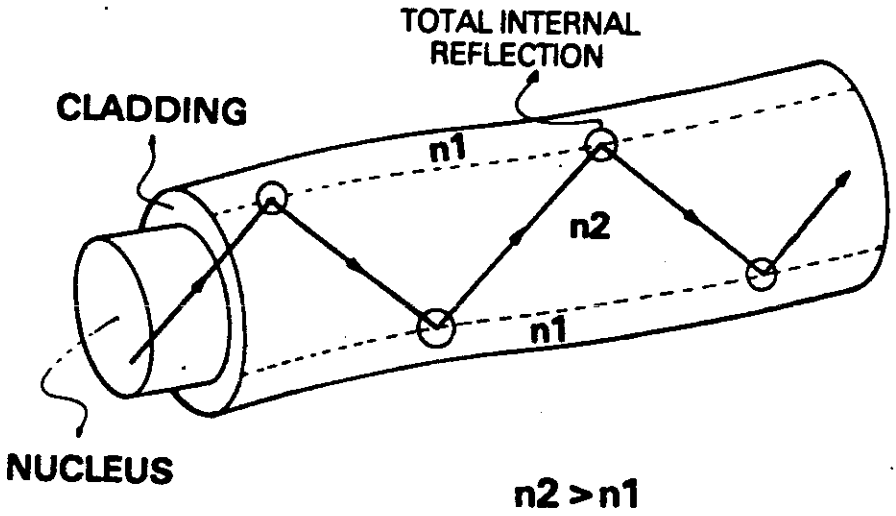

FIGURE 7

abc xtal

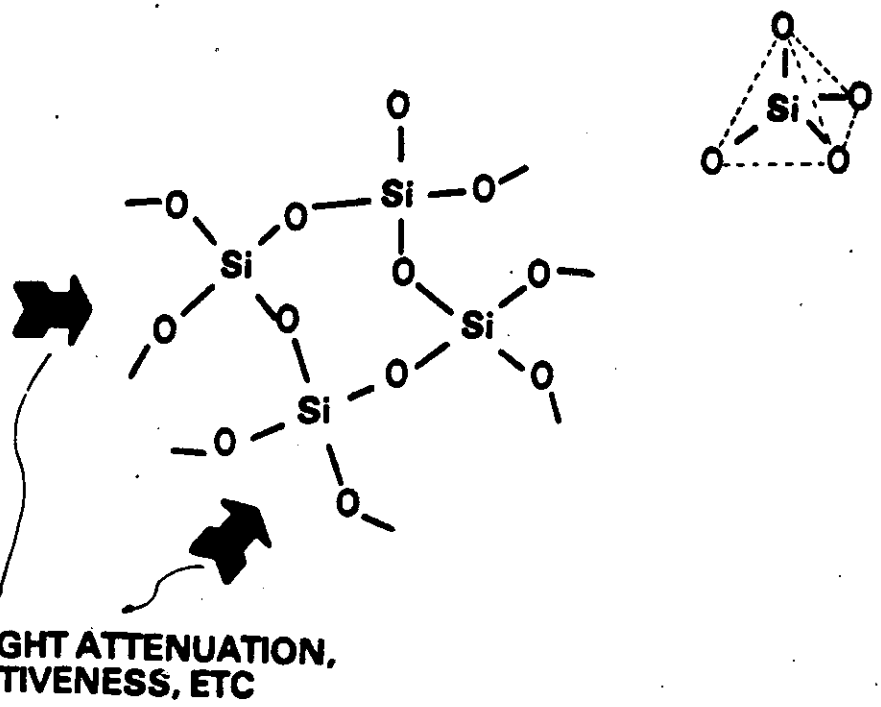

FIGURE 8

abc xtal

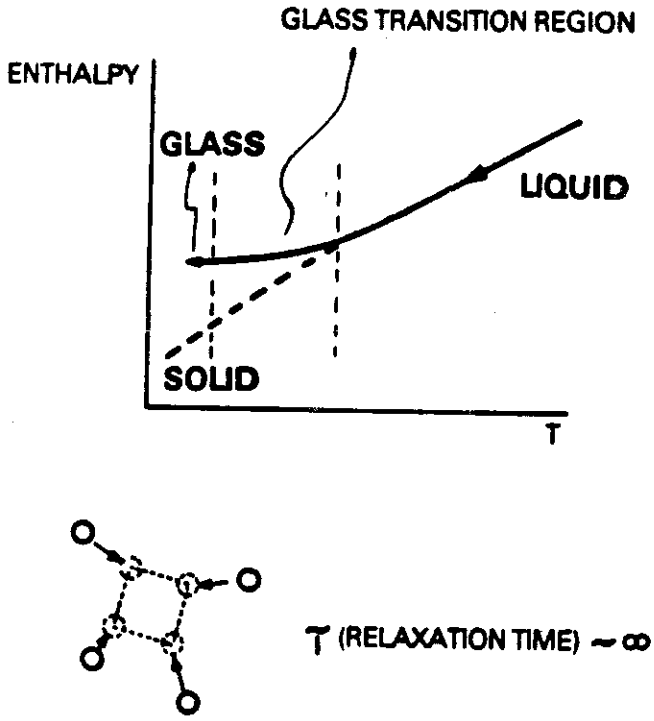

FIGURE 9

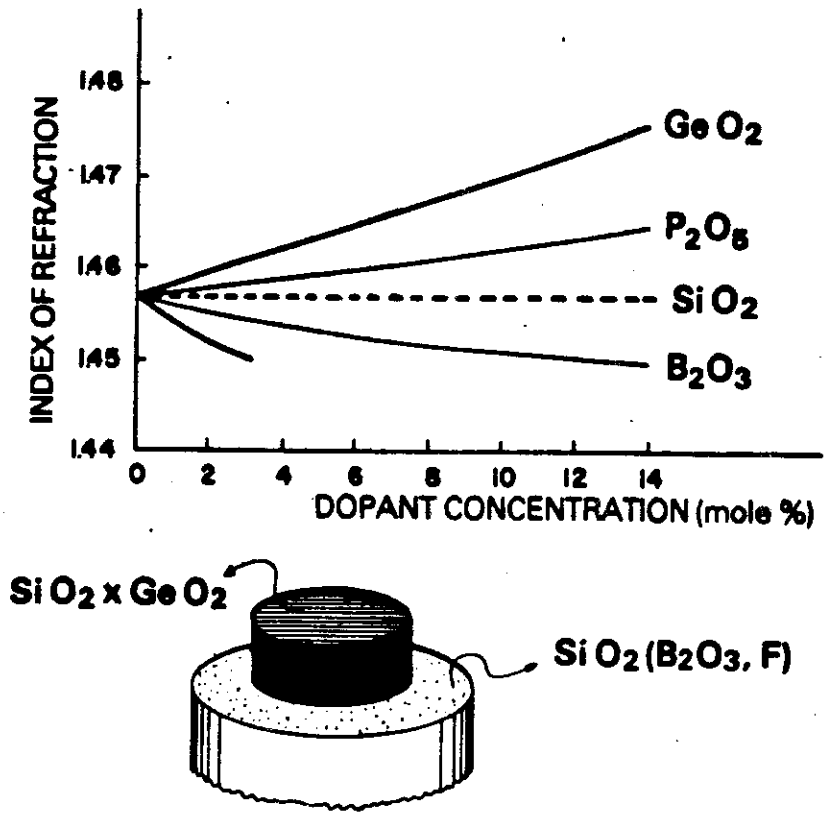

FIGURE 10

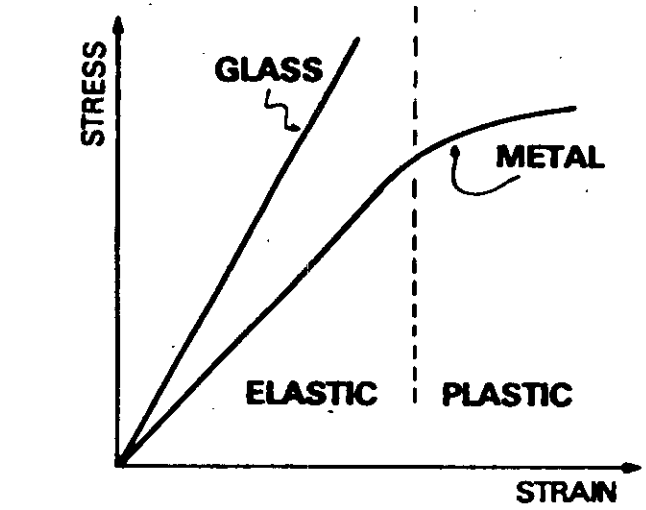

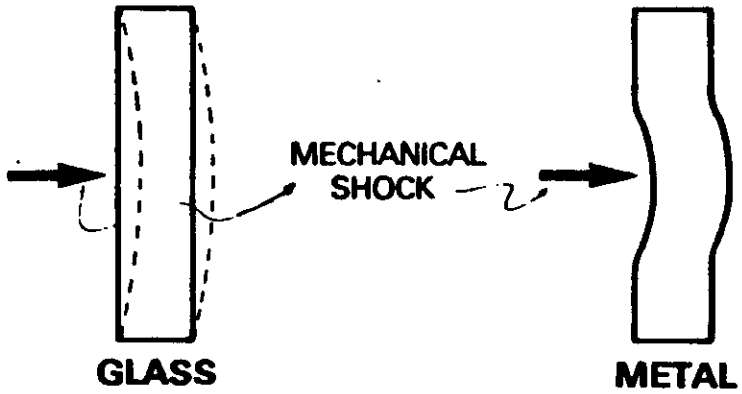

FIGURE 11

abc xtal

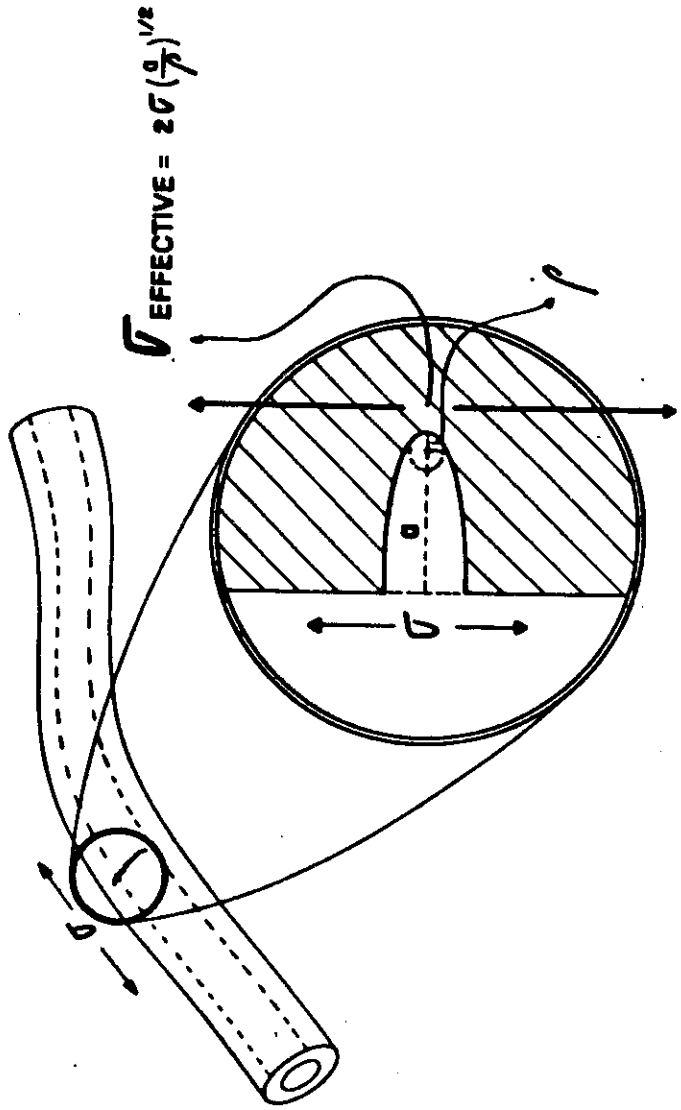

FIGURE 12

abc xtal

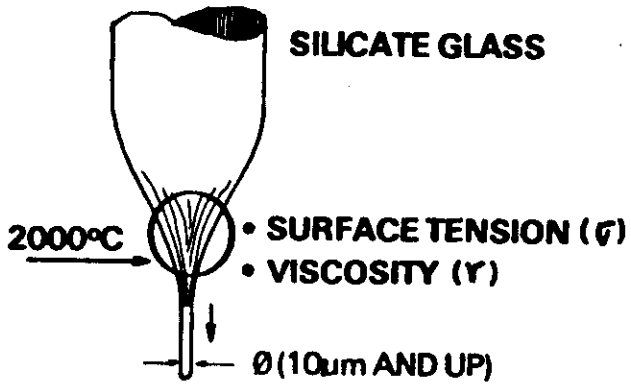

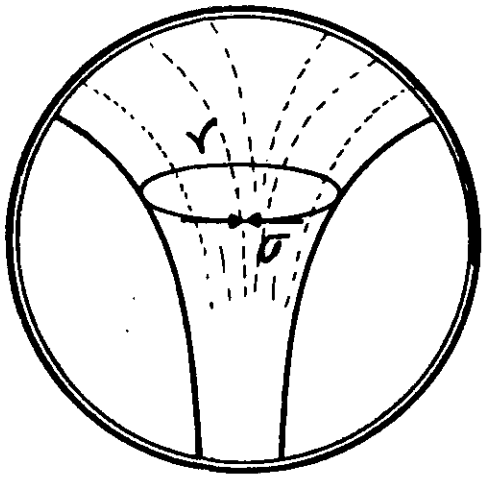

FIGURE 13

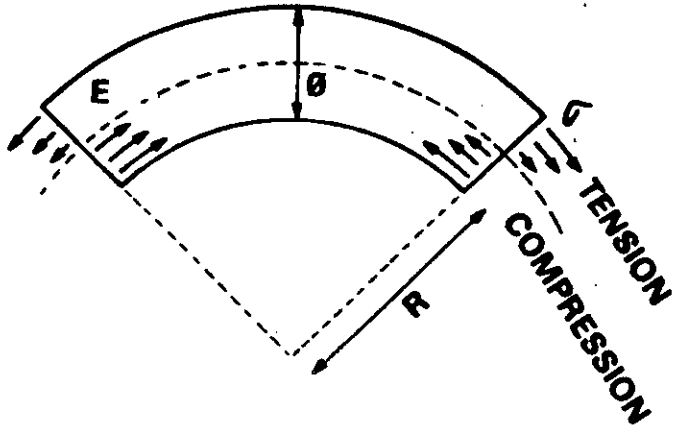

$$R_R = \emptyset \left[\frac{E}{2\sigma_R} - \frac{1}{2} \right]$$

$E = 7 \times 10^3 \text{ kgf/mm}^2$

$\sigma_R = 4 \times 10^2 \text{ kgf/mm}^2$

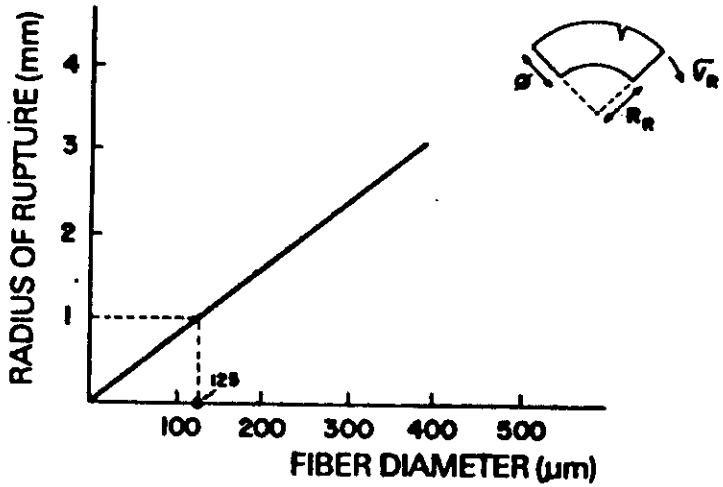

FIGURE 14

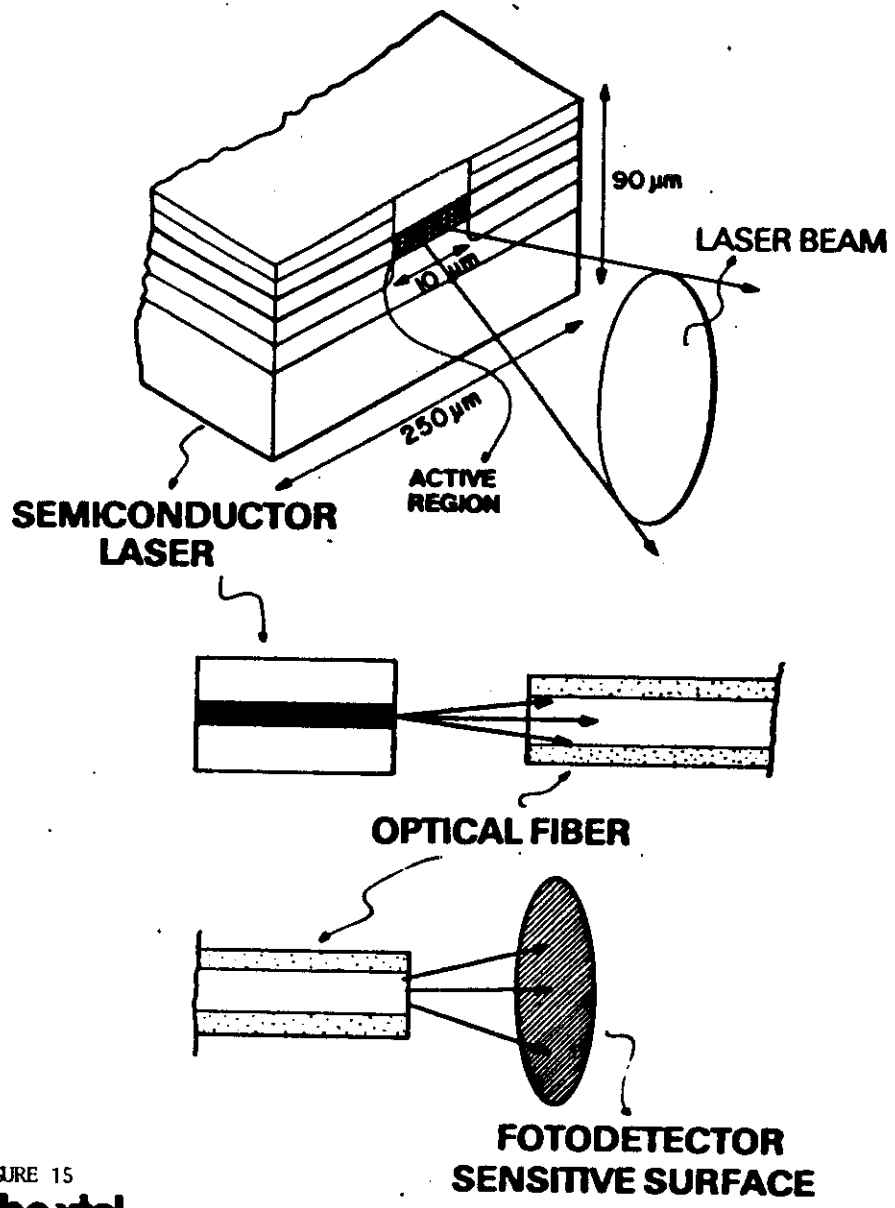

FIGURE 15

abc xtal

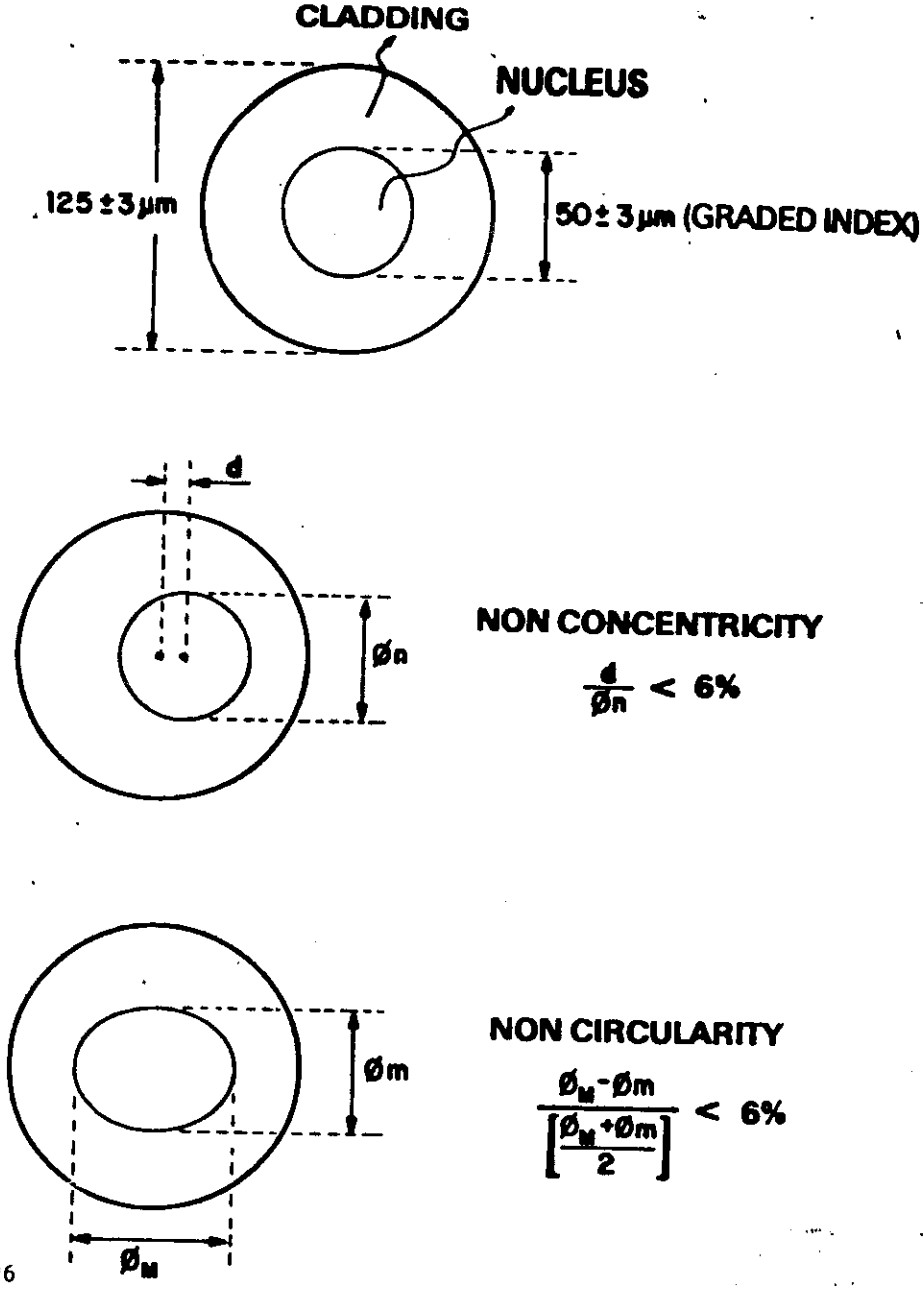

FIGURE 16

abc xtal

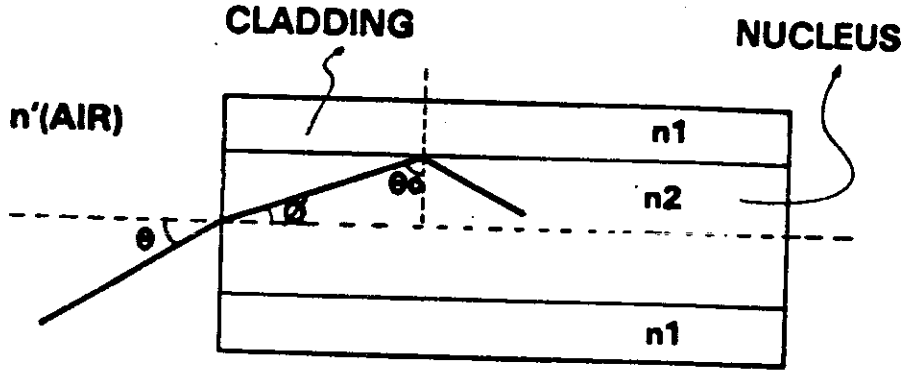

$$n' \sin \theta = n2 \sin \emptyset\ 2$$

$$\theta c = \text{arc. sin} \left(\frac{n1}{n2} \right)$$

$$N.A. = \left[n_2^2 - n_1^2 \right]^{1/2}$$

FIGURE 17

abc xtal

abc xtal

FIGURE 18

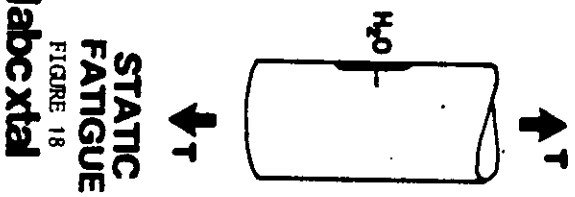

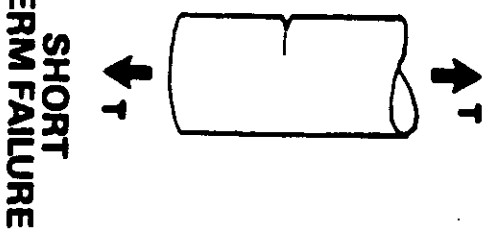

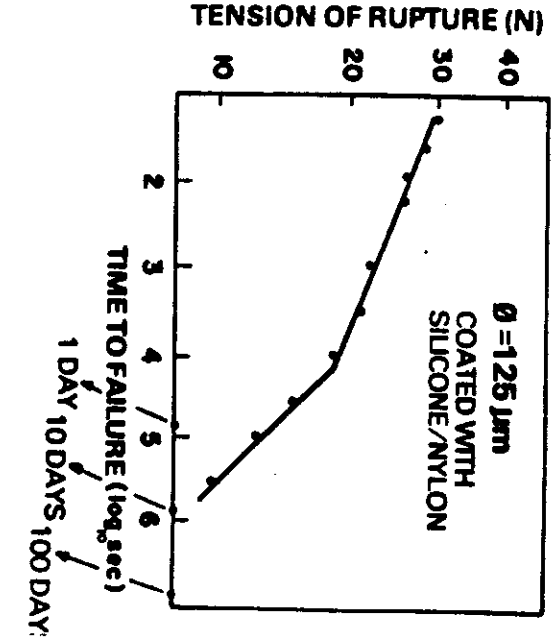

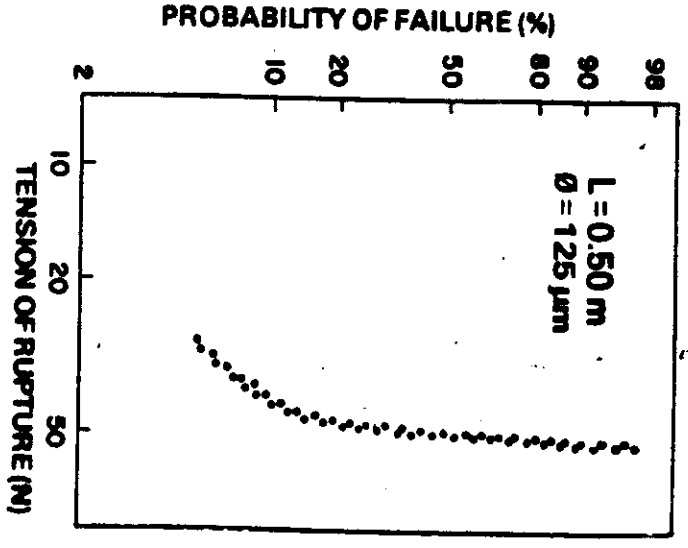

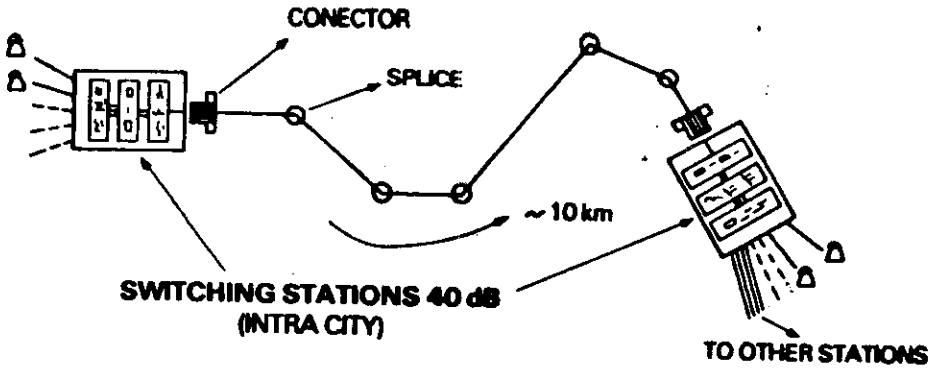

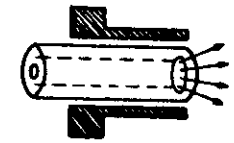

CONECTOR LOSS ~1 dB

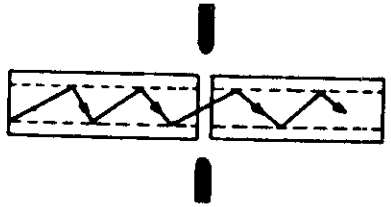

SPLICE LOSS ~0.2 dB

2 CONECTORS	2dB
SPLICING	0.2 dB/km
AGING	6 dB
OPTICAL FIBER	3 dB/km

FIGURE 19

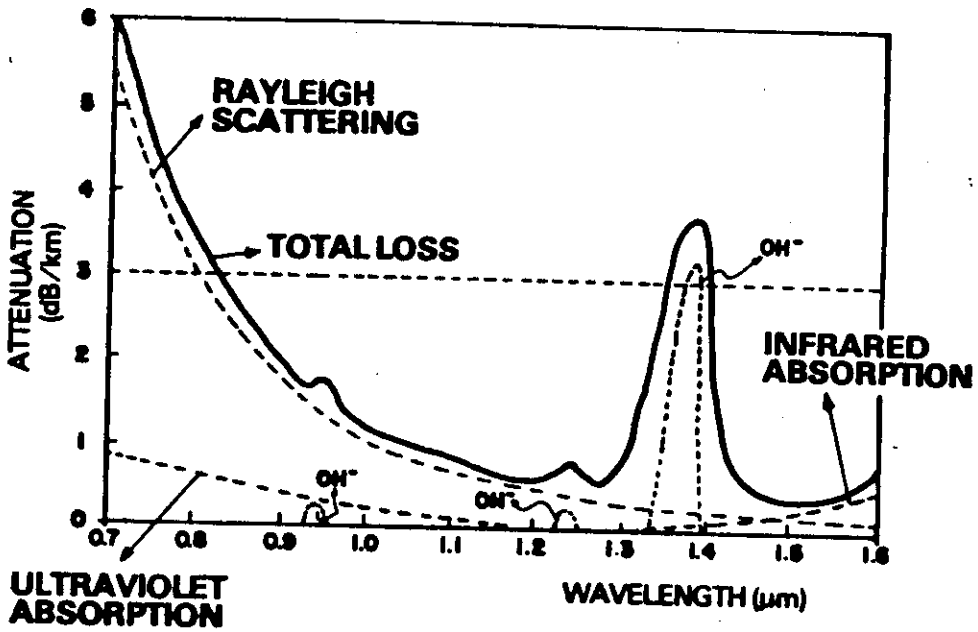

0.83 μm	Al Ga As LASER
1.3 μm - 1.55 μm	InGaAsP LASER

FIGURE 20

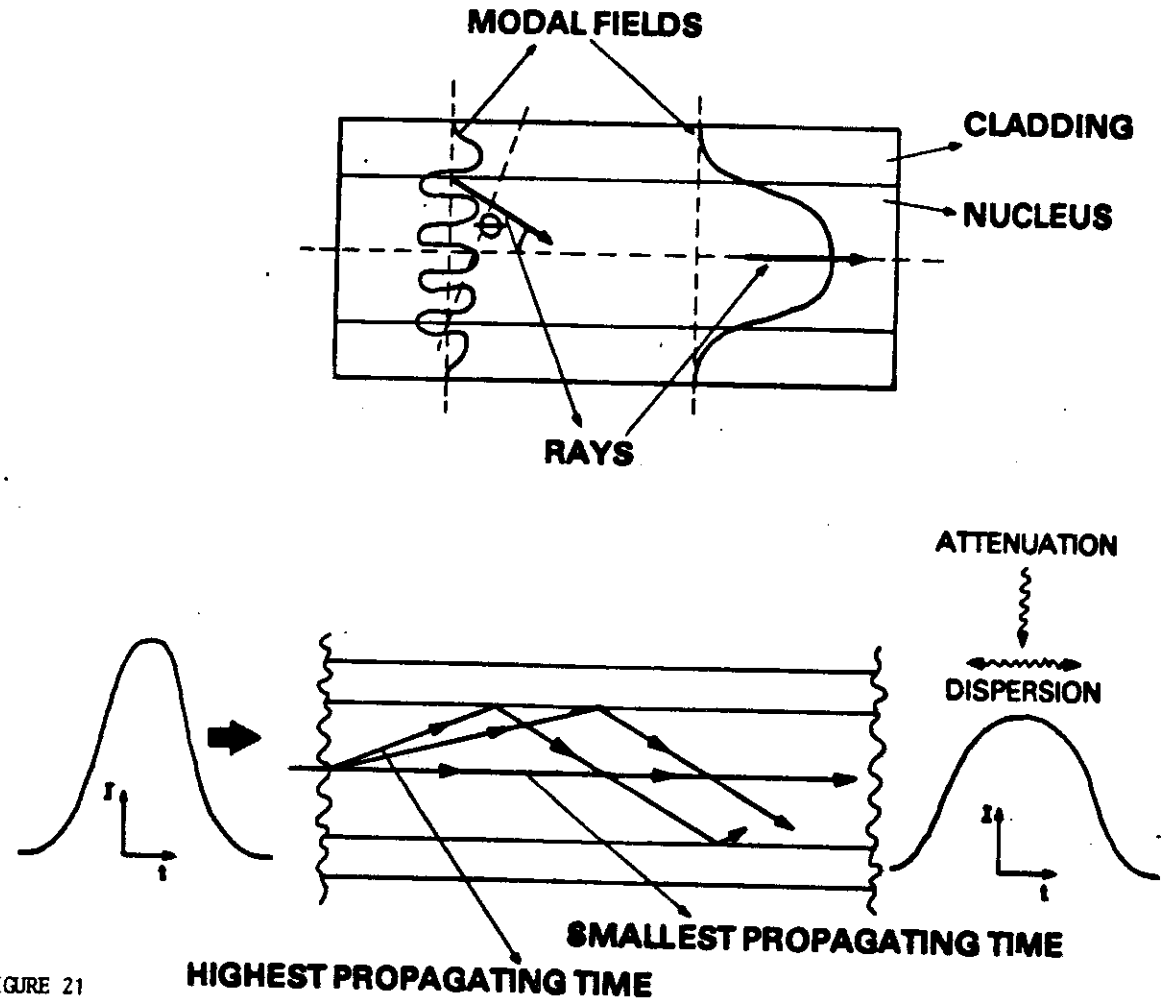

FIGURE 21

abc xtal

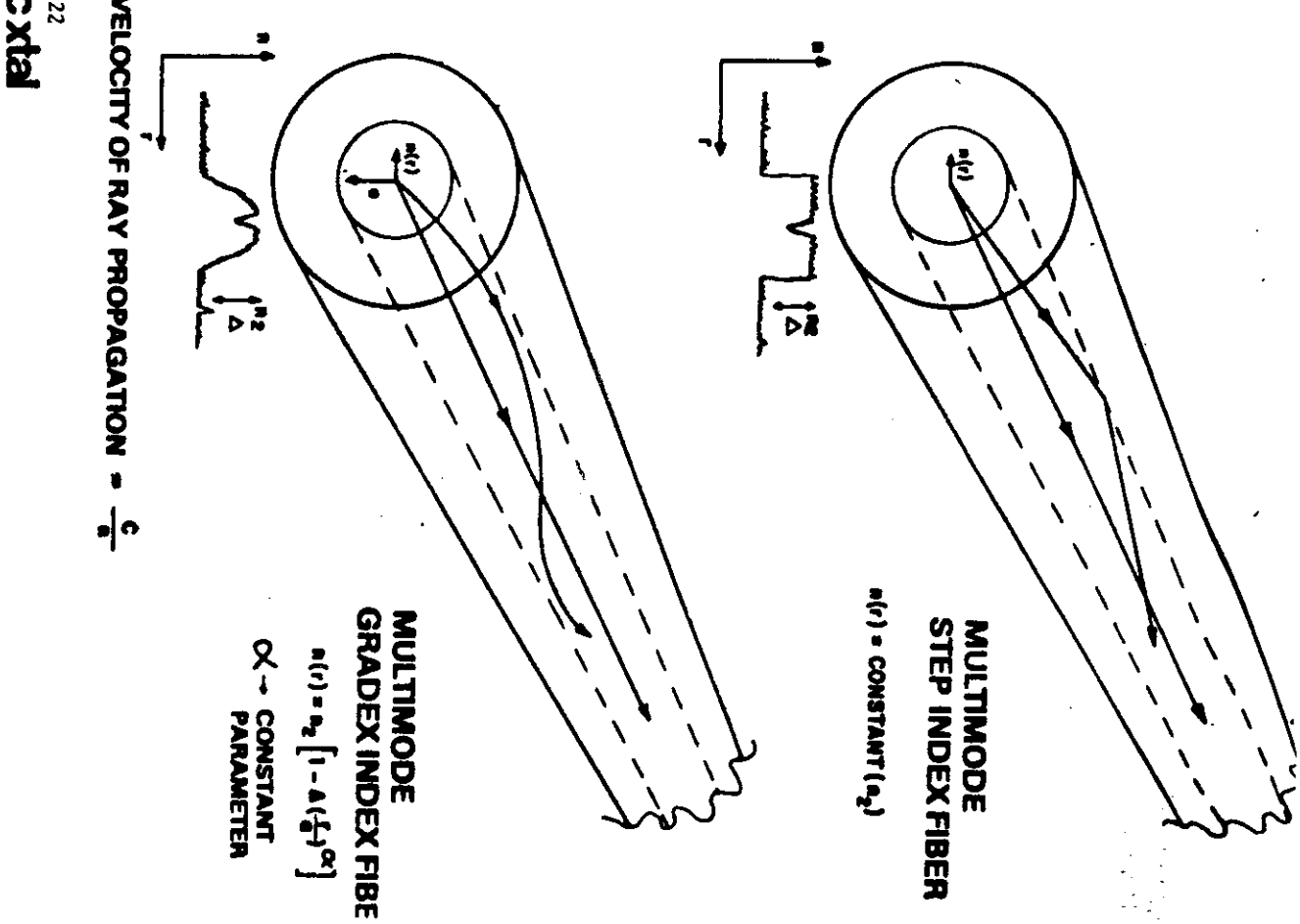

FIGURE 22

abc xtal

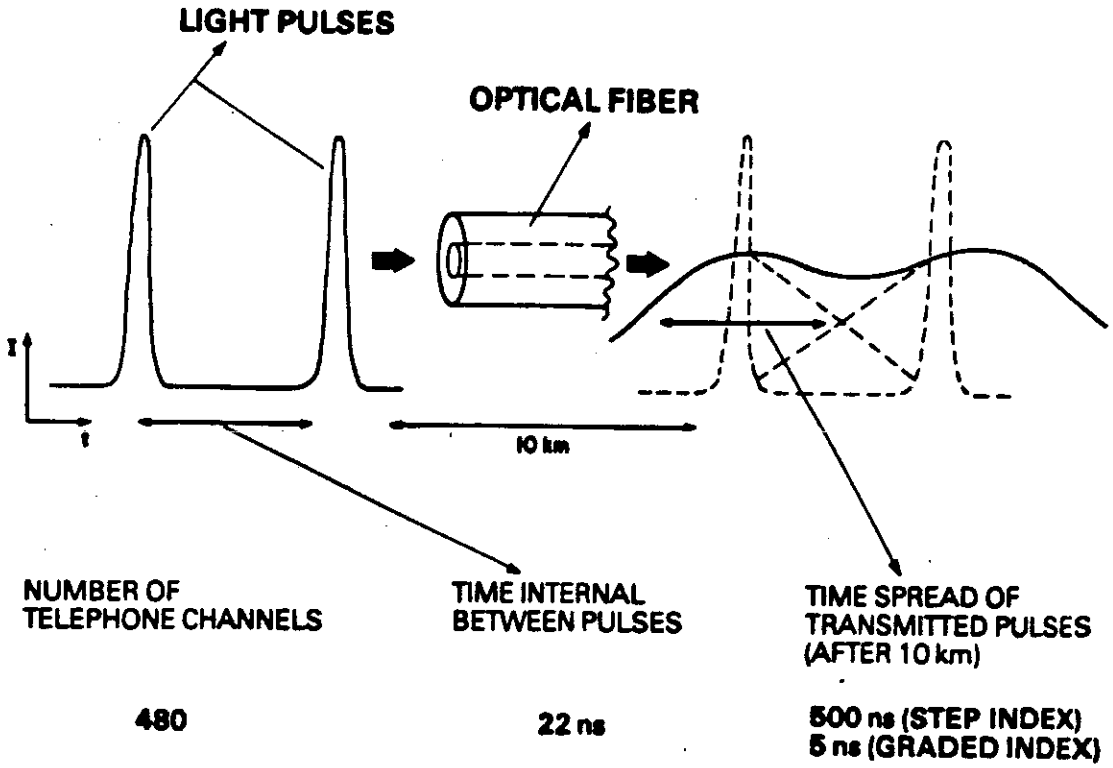

FIGURE 23

abc xtal

FIGURE 24

abc xtal

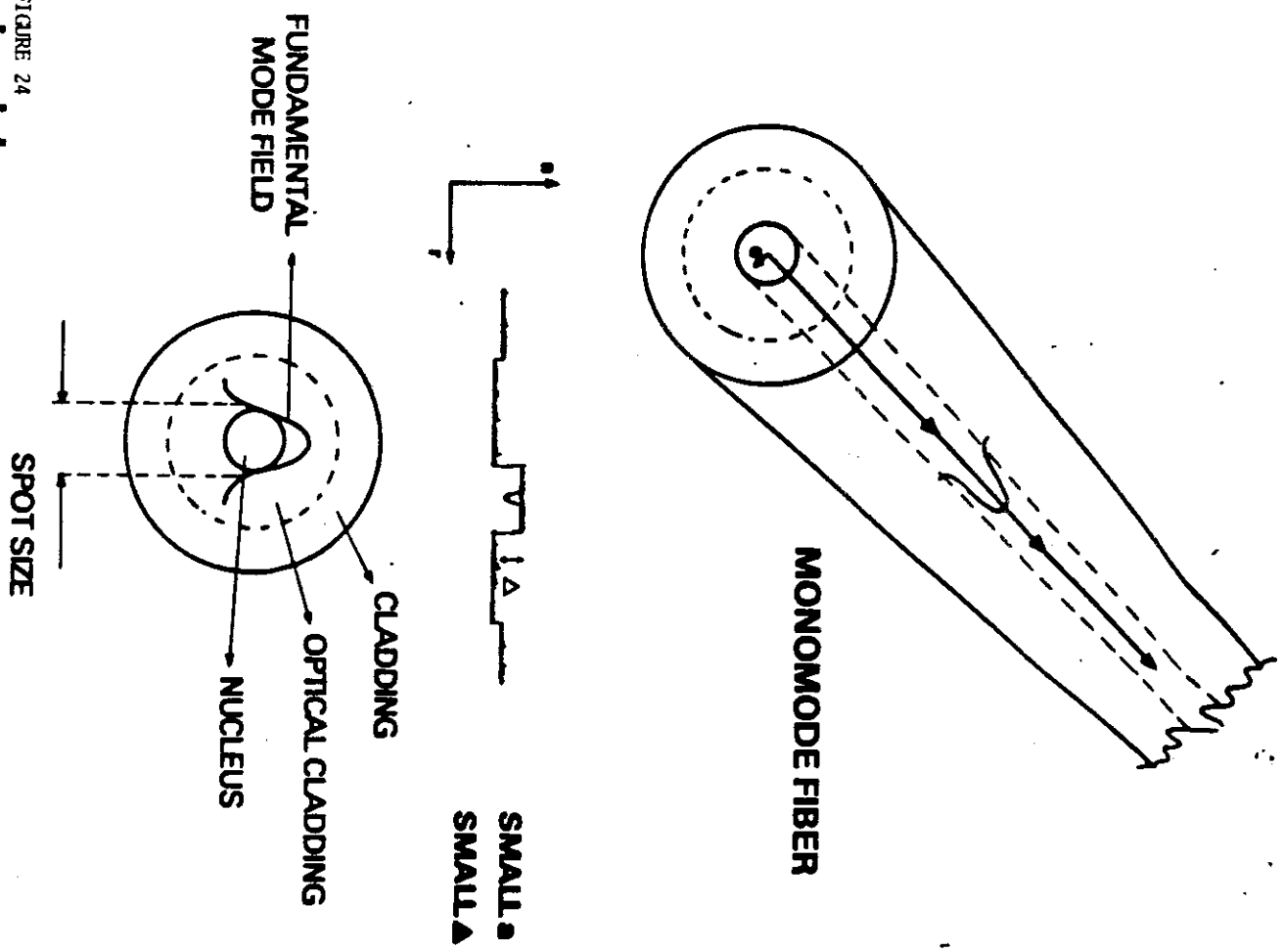

SILICA GLASS

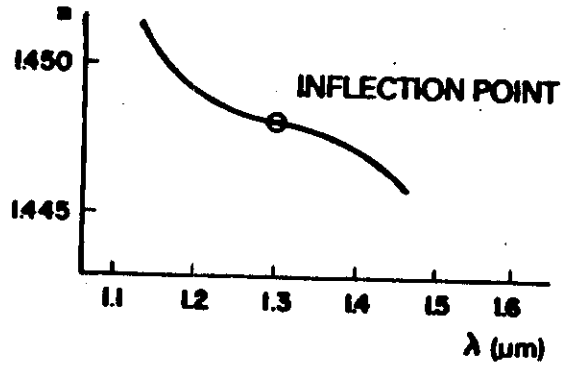

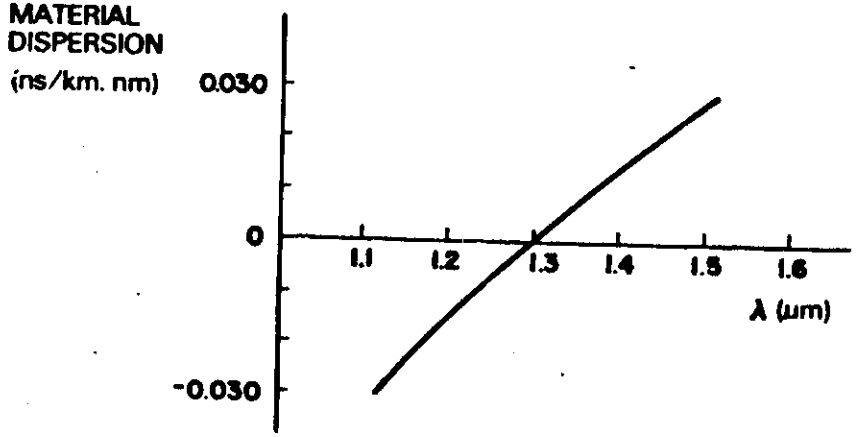

$$\frac{1}{L}\frac{dT_m}{d\lambda} = -\frac{1}{c}\lambda\frac{d^2n}{d\lambda^2}$$

FIGURE 25

abc xtal

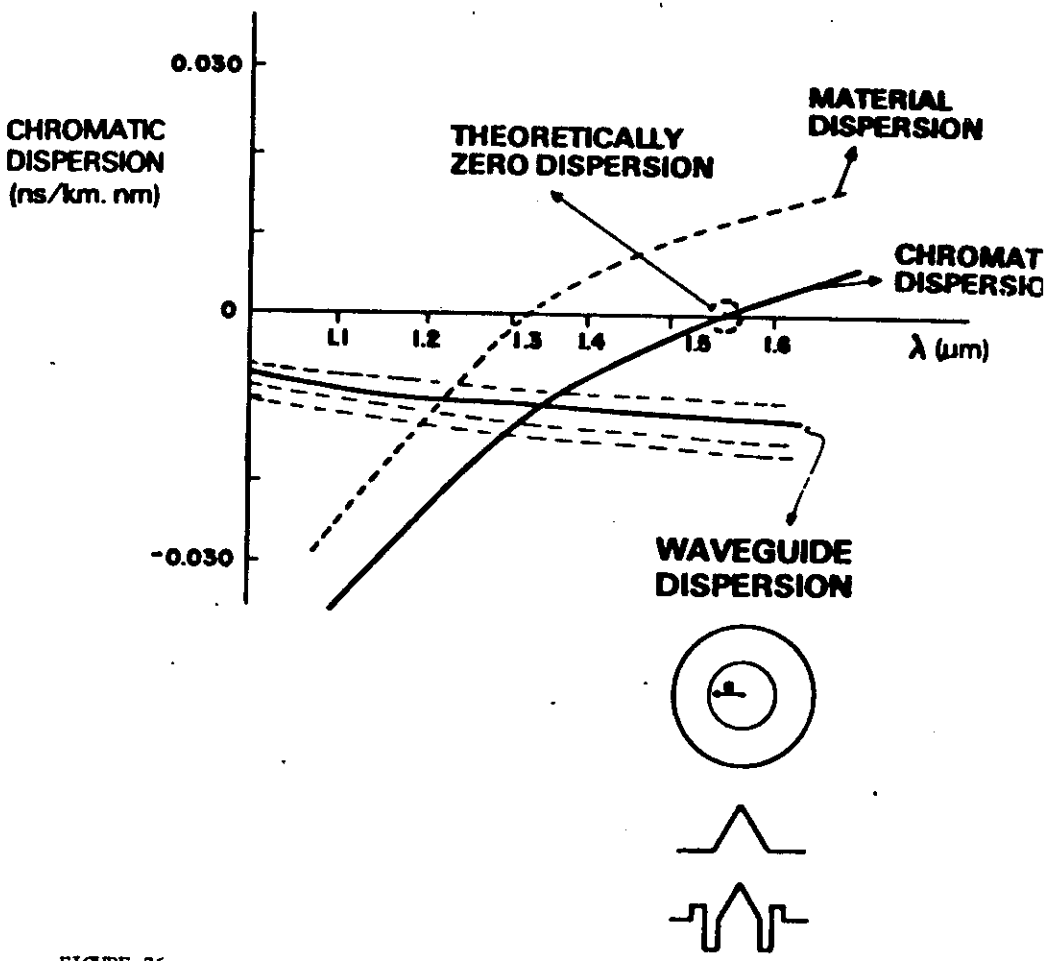

FIGURE 26

abc xtal

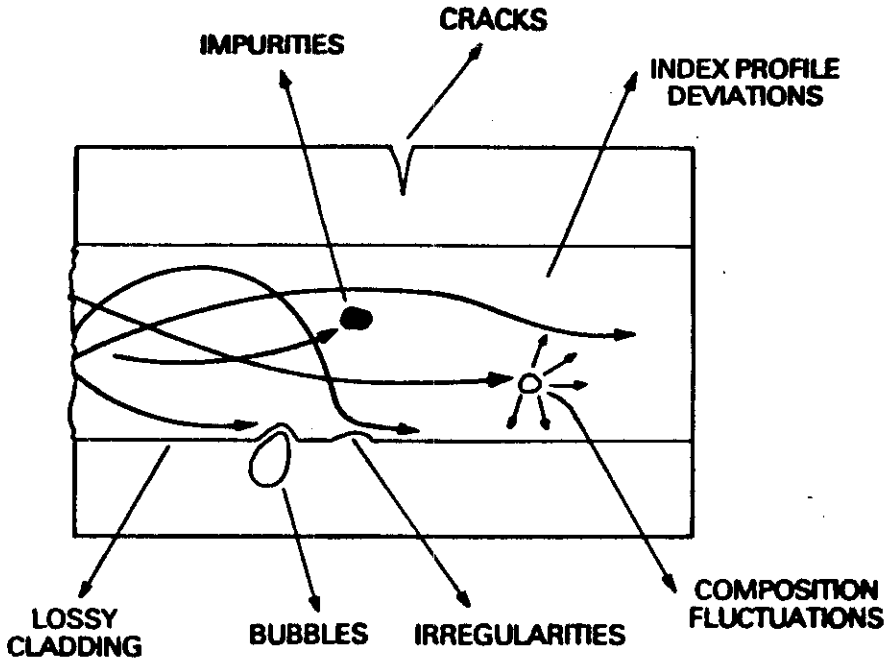

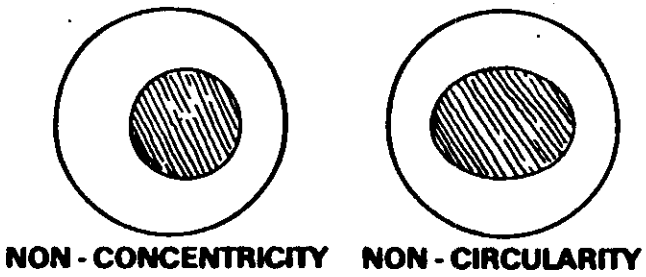

FIGURE 27

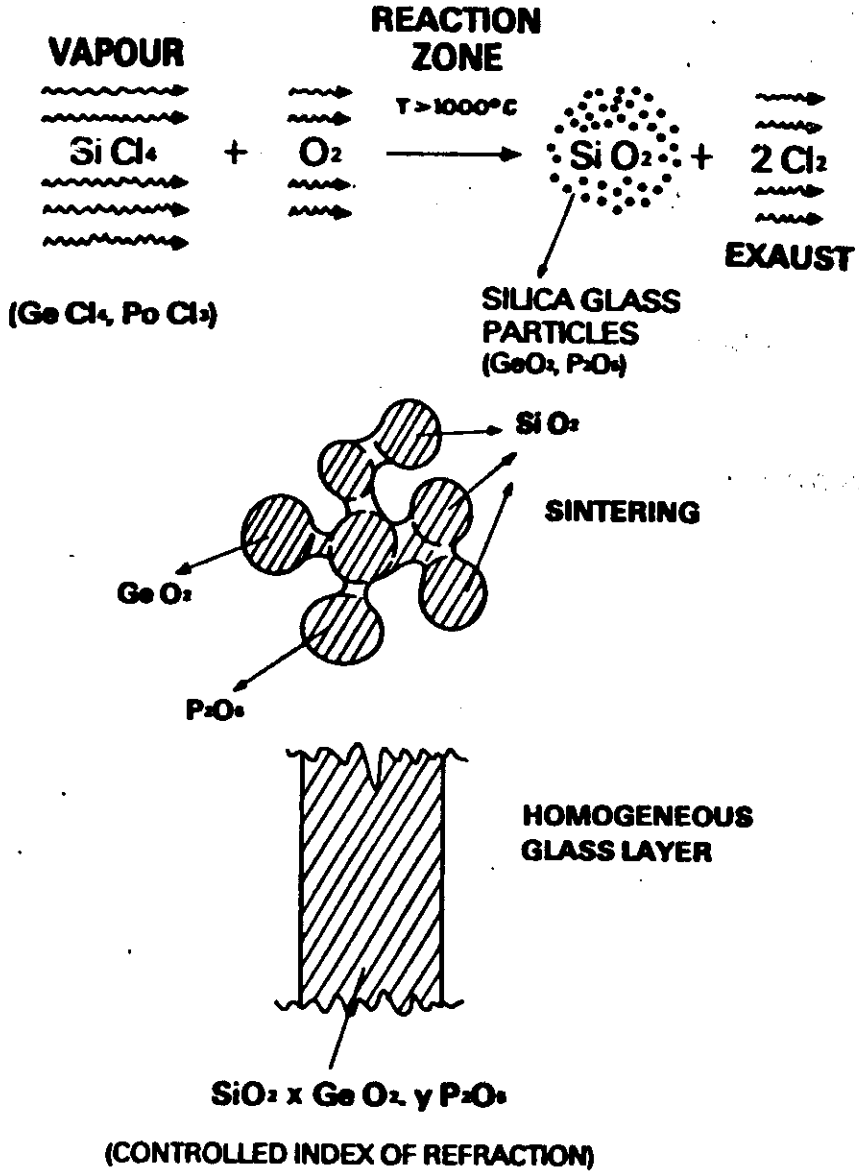

FIGURE 28

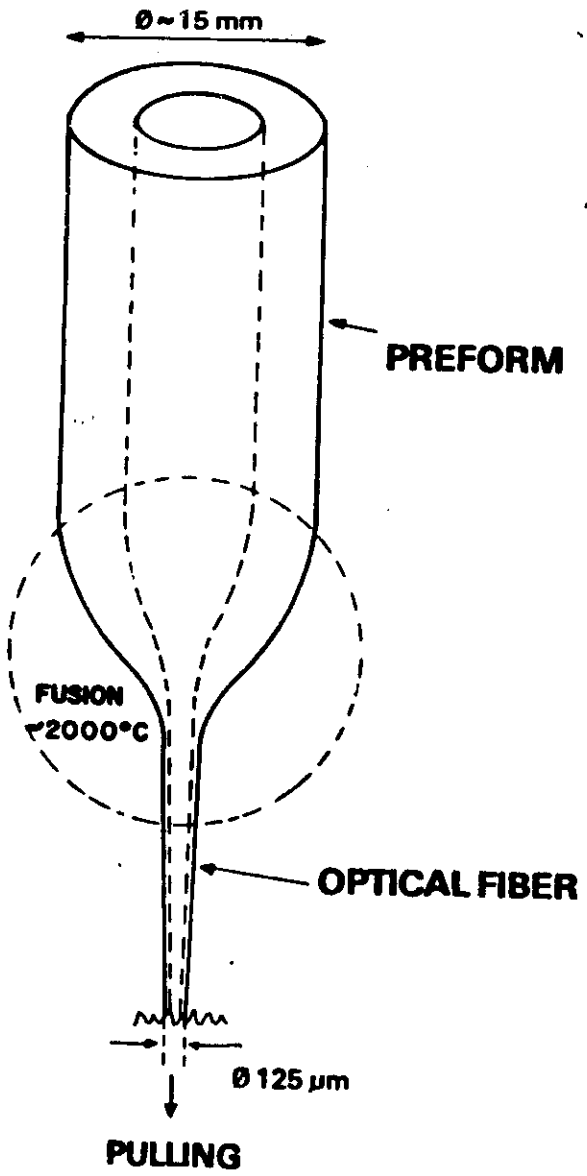

FIXED PARAMETER ON 1st STAGE

- NUCLEUS/CLADDING DIAMETER PROPORTION
- INDEX PROFILE
- MATERIAL STRUCTURE AND PURITY

POSSIBLE VARIATIONS ON 2nd STAGE

- FINAL DIAMETER AND TOLERANCES
- MECHANICAL STRENGTH

FIGURE 29

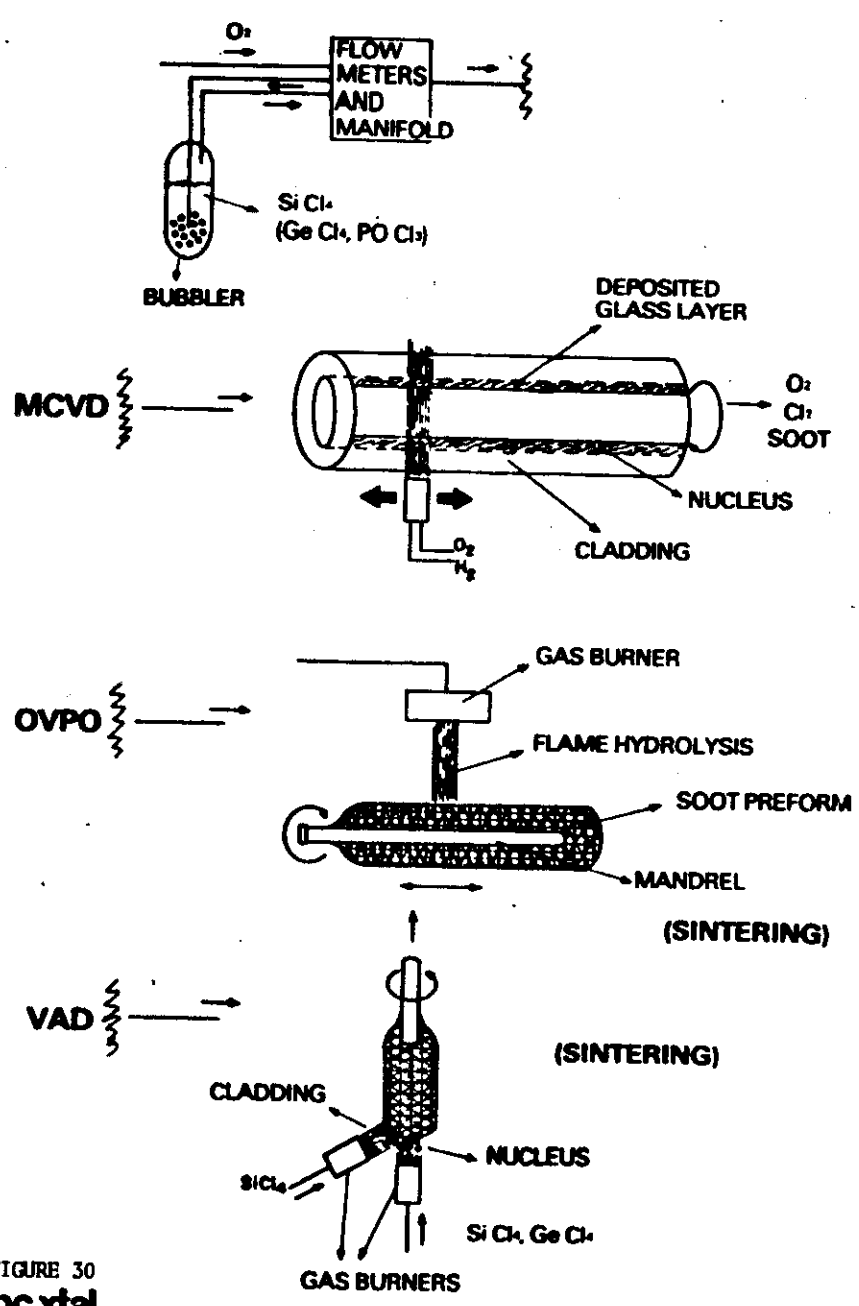

FIGURE 30

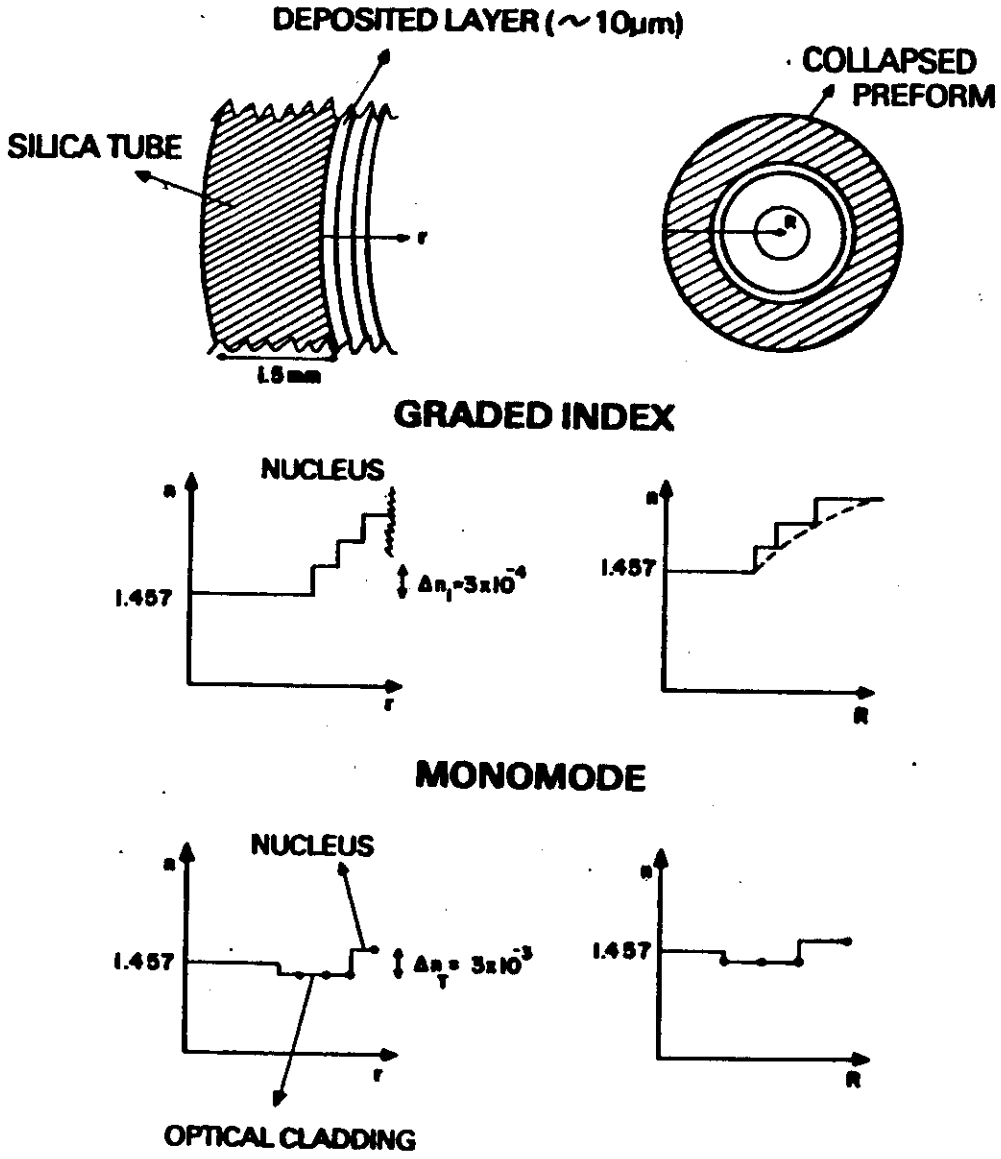

FIGURE 31

abc xtal

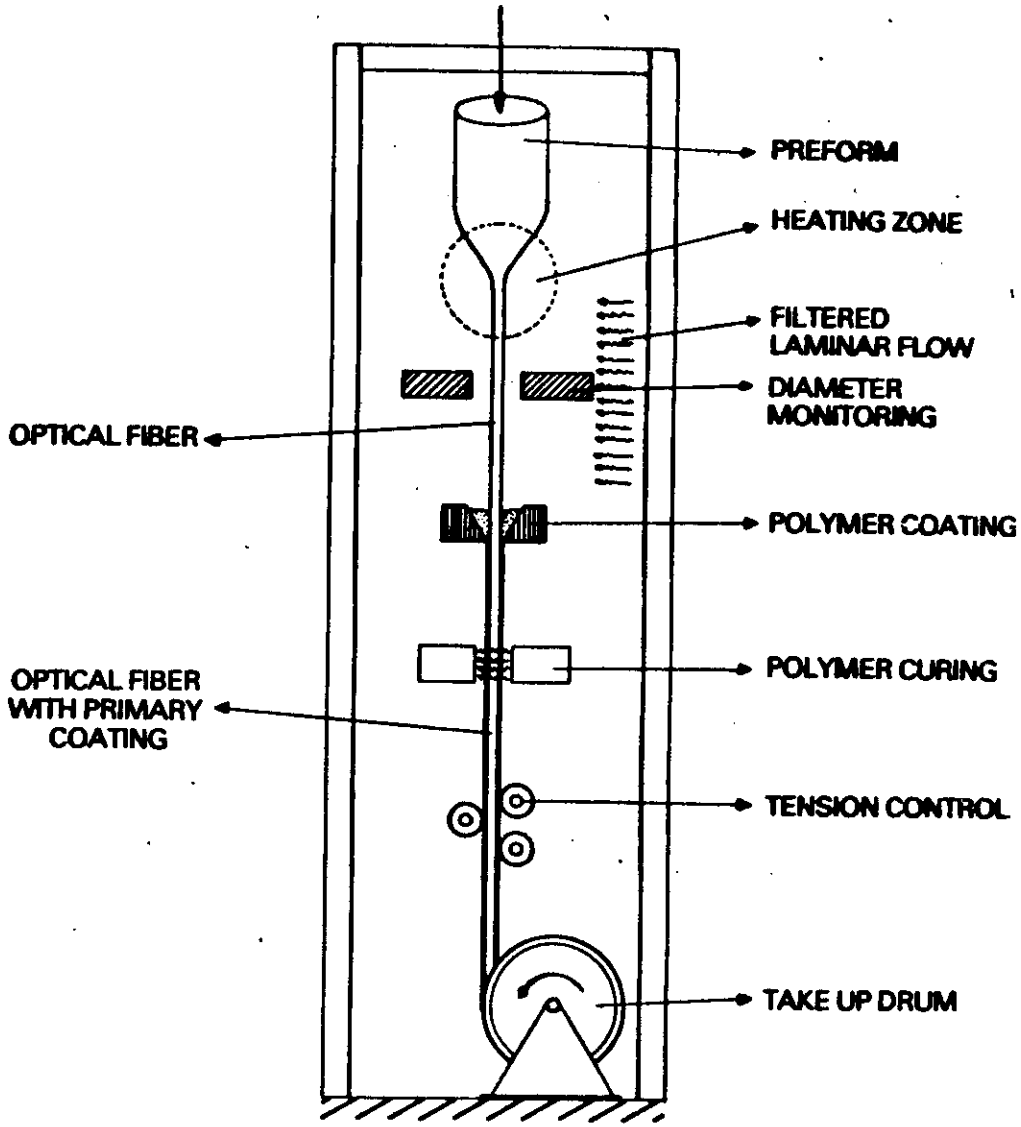

FIGURE 32

abc xtal